

# **Analysis of Spatial Patterns and Dynamics in Ecological Systems using Cellular Automata Models**

Insights from Percolation Theory and Phase  
Transitions

A Thesis submitted for the completion of  
requirements for the degree of

**Bachelor of Science (Research)**

by

**Chandan R T**

Undergraduate Programme  
Indian Institute of Science



Under the supervision of

**Prof. Vishwesha Guttal**

Center for Ecological Sciences, Indian Institute of Science

**Prof. Sriram Ramaswamy**

Department of Physics, Indian Institute of Science



# Certificate

I hereby certify that Chandan R T, a fourth-year undergraduate student of the Bachelor of Science (Research) program at IISc, has worked under my supervision from June 2022 to April 2023. He worked on the analysis of spatial patterns and dynamics in ecological systems using cellular automata models, utilizing insights from percolation theory and phase transitions. After going through his thesis, I have found it to be adequate for fulfilling the requirements of his BS (Research) degree.



11.04.2023

---

**Dr. Vishwesha Guttal**  
Centre for Ecological Sciences  
Department of Biological Sciences  
Indian Institute of Science

# Declaration

I, Chandan R T, hereby declare that the substance contained in this thesis represents original work undertaken by me at the Centre for Ecological Sciences, Department of Biological Sciences, Indian Institute of Science, between June 2022 and April 2023. I have made maximal efforts to acknowledge the efforts (of literary, empirical, and computational nature) of other members of the scientific community to the best of my knowledge. Any omission is unintentional and deeply regretted.

R.T. Chandan

.....  
**Chandan R T**  
Bachelor of Science (Research) Program  
Physics Major  
Indian Institute of Science



.....  
**Prof. Sriram Ramaswamy**  
Department of Physics  
Indian Institute of Science

# Acknowledgements

I would like to express my heartfelt gratitude to everyone who supported me throughout my journey at this institute. Firstly, I would like to thank my thesis supervisor, Dr. Vishwesha Guttal, for his guidance and mentorship throughout this thesis. His agreement to being my thesis guide removed a major source of anxiety for me, during a time when I was highly uncertain about my future prospects. His lab proved to be a highly conducive environment for research. I would also like to thank my colleagues at the lab: Abheepsa, Akshay, Apuroopa, Ashish, Cassandre, Shikhara, Shuaib, Tanveen, Viraj and Vivek, for their fruitful interactions. I would like to thank Arshed in particular for helping me with myriad issues on optimization and usage of computing resources.

I would like to thank the members of our close-knit friend group: Aditya Iyer, Chinmay Haritas, Raj Mehta and Sai Shyam, for their friendship and support throughout the course of this degree.

I would also like to thank my parents, sister and extended family members for their support, not only during this degree but throughout my life.

Finally, I would like to thank the UG department at IISc, for providing me the opportunity to study at one of the most reputed institutes in India. I also thank the Department of Science and Technology for funding the KVPY scholarship, of which I am a recipient.

# Abstract

The services rendered by myriad ecosystems on planet Earth are required for the sustenance of living organisms. The diversity and interactions amongst organisms of many species provide much-needed resilience against mass extinction events. However, due to plethora of anthropogenic activities, ecosystems are collapsing at an alarming rate. These ecological disasters come with economic losses that are mostly borne by weaker sections of the society.

Recovery of ecosystems is possible, albeit an arduous task. This is further complicated by phenomenon like *hysteresis*. Instead of dealing with the consequences, theoretical ecologists strive to devise something known as *early warning signals*: certain behaviour(s) showcased by ecosystems that are poised to undergo collapse. In that way, vulnerable ecosystems can be identified, and precautionary steps can be taken to prevent ecological disasters.

In this thesis, we study the patterns and dynamics of a subset of ecosystems called *patchy ecosystems*. Firstly, we review the early warning signals that have already been studied in literature. Then, we simulate various models whose behaviour is similar to that of patchy ecosystems, and we track the fine-grained dynamics of patch sizes. Based on this, we identify and explain two novel behaviours that can be added to the repertoire of early warning signals for patchy ecosystems.

**Keywords:** Early warning signals, non-linear dynamics, bifurcations, self-organization, percolation theory, phase/ecological transitions, power-law behaviour

# List of Figures

1.1	Examples of power-law clustering in different patchy ecosystems . . . . .	1
1.2	Bifurcation diagram of the harvesting/predation model . . . . .	3
1.3	Feedback mechanisms in the global climate system . . . . .	4
1.4	Visual aid for understanding Von-Neumann clusters . . . . .	6
1.5	Comparison of normalized power-law ( $x^{-\beta}$ ), exponential ( $e^{-x}$ ) and Gaussian ( $e^{-x^2}$ ) distributions . . . . .	7
1.6	Depiction of a percolating cluster . . . . .	8
1.7	Population time series for different values of $r$ . . . . .	11
1.8	Increase in variance due to critical slowing down . . . . .	12
2.1	Schematic of TDP model . . . . .	16
2.2	Behaviour of TDP model for various values of $q$ . . . . .	17
2.3	Phase diagram of TDP model . . . . .	18
2.4	Percolation thresholds of TDP model . . . . .	18
2.5	Percolation transitions of TDP model . . . . .	19
2.6	Bifurcation diagram of Scanlon's model . . . . .	21
2.7	Variation of percolation threshold with increasing radius of influence in Scanlon's model . . . . .	21
2.8	Variation of percolation threshold with increasing immediacy in Scanlon's model . . . . .	22
2.9	Percolation transition in static null model . . . . .	23
2.10	Percolation transition in dynamic null model . . . . .	24
3.1	An example of two lattices that differ by only one update . . . . .	25

4.1	Variation of cluster size distribution across the $q = 0$ percolation threshold of TDP model . . . . .	33
4.2	Cluster size distribution across the percolation threshold . . . . .	34
4.3	Variation of cluster size distribution across the $q = 0.25$ percolation threshold of TDP model . . . . .	34
4.4	Variation of cluster size distribution across the $q = 0.5$ percolation threshold of TDP model . . . . .	35
4.5	Variation of cluster size distribution across the $q = 0.75$ percolation threshold of TDP model . . . . .	35
4.6	Variation of cluster size distribution across the $q = 0.92$ percolation threshold of TDP model . . . . .	36
4.7	Variation of cluster dynamics across the $q = 0$ percolation threshold of TDP model . . . . .	37
4.8	Variation of cluster dynamics across the $q = 0.25$ percolation threshold of TDP model . . . . .	37
4.9	Variation of cluster dynamics across the $q = 0.5$ percolation threshold of TDP model . . . . .	38
4.10	Variation of cluster dynamics across the $q = 0.75$ percolation threshold of TDP model . . . . .	38
4.11	Variation of cluster dynamics across the $q = 0.92$ percolation threshold of TDP model . . . . .	39
4.12	Variation of drift and diffusion across the $q = 0$ percolation threshold of TDP model . . . . .	40
4.13	Variation of drift and diffusion across the $q = 0.25$ percolation threshold of TDP model . . . . .	41
4.14	Variation of drift and diffusion across the $q = 0.5$ percolation threshold of TDP model . . . . .	41
4.15	Variation of drift and diffusion across the $q = 0.75$ percolation threshold of TDP model . . . . .	42
4.16	Variation of drift and diffusion across the $q = 0.92$ percolation threshold of TDP model . . . . .	42
4.17	Comparison between results of TDP and null model across the $q = 0$ percolation threshold . . . . .	44

4.18 Comparison between results of TDP and null model across the $q = 0.25$ percolation threshold . . . . .	44
4.19 Comparison between results of TDP and null model across the $q = 0.5$ percolation threshold . . . . .	45
4.20 Comparison between results of TDP and null model across the $q = 0.75$ percolation threshold . . . . .	45
5.1 Decay of power-law clustering across near the critical threshold of $q = 0$ . . . . .	48
5.2 Decay of power-law clustering across near the critical threshold of $q = 0.25$ . . . . .	49
5.3 Decay of power-law clustering across near the critical threshold of $q = 0.5$ . . . . .	50
5.4 Exponential behaviour of cluster dynamics near critical threshold of $q = 0$ . . . . .	52
5.5 Increase in goodness of exp fit below percolation threshold of $q = 0$ . . . . .	52
5.6 Exponential behaviour of cluster dynamics near critical threshold of $q = 0.25$ . . . . .	53
5.7 Increase in goodness of exp fit below percolation threshold of $q = 0.25$ . . . . .	53
5.8 Exponential behaviour of cluster dynamics near critical threshold of $q = 0.5$ . . . . .	54
5.9 Increase in goodness of exp fit below percolation threshold of $q = 0.5$ . . . . .	54
5.10 Variation in fixed point near the critical threshold of $q = 0$ . . . . .	56
5.11 Decrease in critical cluster size near the critical threshold of $q = 0$ . . . . .	56
5.12 Variation in fixed point near the critical threshold of $q = 0.25$ . . . . .	57
5.13 Decrease in critical cluster size near the critical threshold of $q = 0.25$ . . . . .	57
5.14 Variation in fixed point near the critical threshold of $q = 0.5$ . . . . .	58
5.15 Decrease in critical cluster size near the critical threshold of $q = 0.5$ . . . . .	58
5.16 Cluster size distribution in Scanlon's model . . . . .	59
5.17 Cluster dynamics in Scanlon's model . . . . .	60
5.18 Drift and diffusion terms in Scanlon's model . . . . .	60
5.19 The global picture . . . . .	61

# Contents

<b>Acknowledgements</b>	<b>iii</b>
<b>Abstract</b>	<b>iv</b>
<b>List of Figures</b>	<b>vii</b>
<b>1 Introduction</b>	<b>1</b>
1.1 Patchy Ecosystems . . . . .	1
1.2 Abrupt Transitions and Hysteresis . . . . .	2
1.3 Terminology . . . . .	5
1.4 Early Warning Signals in Literature . . . . .	9
1.5 Objectives . . . . .	12
<b>2 Models</b>	<b>14</b>
2.1 Contact Process . . . . .	14
2.2 Tricritical Directed Percolation . . . . .	15
2.3 Scanlon's Model . . . . .	19
2.4 Null Model for Cluster Size Distribution . . . . .	22
2.5 Null Model for Cluster Dynamics . . . . .	22
<b>3 Methods</b>	<b>25</b>
3.1 Cluster Tracking Algorithm . . . . .	25
3.2 Evaluation of Goodness of Power-law Fits . . . . .	29
3.3 Process of SDE Discovery . . . . .	30
<b>4 Results</b>	<b>32</b>

4.1 Cluster Size Distribution . . . . .	33
4.2 Cluster Dynamics . . . . .	36
4.3 SDE Discovery for Cluster Sizes . . . . .	39
4.4 Comparison with Results from Null Models . . . . .	43
<b>5 Discussion</b>	<b>46</b>
5.1 Deviation of cluster size distribution from power-law behaviour near critical thresholds . . . . .	47
5.2 Exponential behaviour of cluster dynamics near critical thresholds . . . . .	51
5.3 Rapid decrease in critical cluster size near critical thresholds . . . . .	55
5.4 Ubiquity of Power-Law Behaviour . . . . .	59
5.5 Concluding Remarks and Future Work . . . . .	61
<b>Bibliography</b>	<b>64</b>

# Chapter 1

## Introduction

### 1.1 Patchy Ecosystems

Ecological systems in nature undergo self-organization. Some systems, like semi-arid vegetation, mussel beds and sea-grasses, showcase spatial patterns that exhibit a power-law distribution in their patch/cluster<sup>1</sup> sizes (figure 1.1). This phenomenon is called *power-law clustering*.

Models of patchy ecosystems that incorporate facilitation mechanisms have been observed to replicate real-world patterns in a better manner [Kéfi et al. (2007b)]. It has been suggested that facilitation is responsible for power-law clustering [Scanlon et al. (2007)].

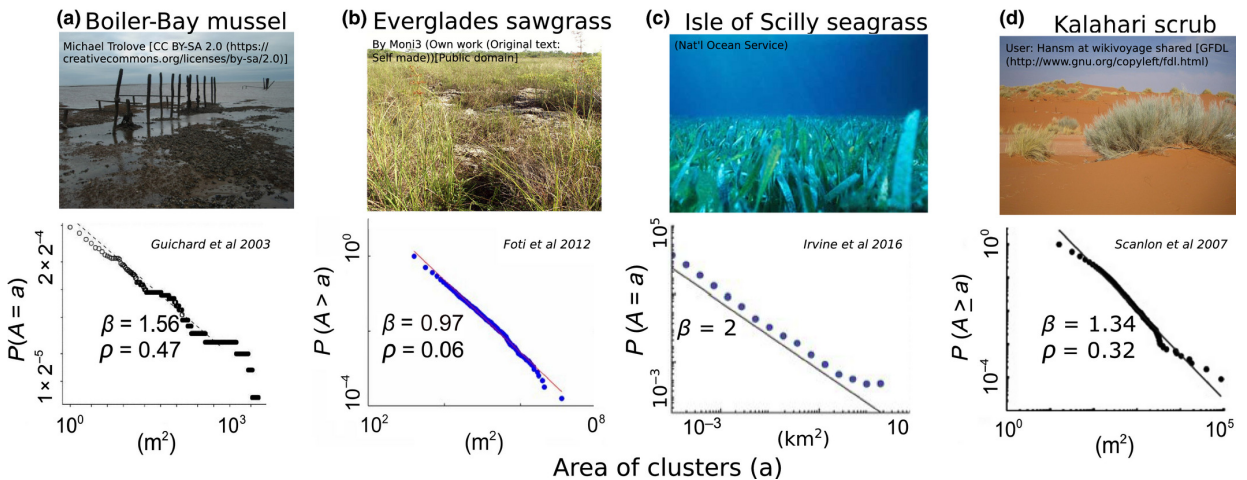


Figure 1.1: Examples of power-law clustering in different patchy ecosystems

The images on top depict the ecosystem in question. The graphs on bottom are log-log plots of the cluster size distribution. Figure taken from [Sankaran et al. (2019)].

Attributions for individual figures have been mentioned in the figure

<sup>1</sup>Note that the terms *cluster* and *patch* can be used interchangeably

## 1.2 Abrupt Transitions and Hysteresis

The dynamics of ecological systems can be modelled using differential equations or cellular automata. The variables of interest may be the population of a species in a given region, or the fraction of a given region that is occupied by vegetation.

If all the entities in the system are assumed to be ‘well-mixed’, and the spatial extent of the system is ignored, then the model is called a *mean-field model*. However, The system’s space can be divided into several regions, with each region having its own set of parameters and neighbouring regions interacting with each other. If the dynamics of this model is described using differential equations, then such coarse-grained models are called *reaction-diffusion models*. An interactive simulation of a reaction-diffusion model can be found [here](#). This sort of coarse-graining is implicit in automata. Refer section 1.3.3 for a description of automata.

Mean-field models, reaction-diffusion models as well as automata showcase a change in the variable(s) of interest as the model parameter(s) are varied. The change may be continuous or abrupt. Such changes are called *phase transitions* or *regime shifts* [May (1977)]. The parameter(s) of the model at which a phase transition takes place is known as *critical point* (if the transition is continuous) or *critical threshold* (if the transition is abrupt).

Consider a generic model that incorporates a density dependent population growth as well as the effect of harvesting/predation. We can use this to model the population of insects in the presence of predators [Ludwig et al. (1978)], or a population of fish in the presence of harvesting. We consider the former case. Let  $X$  denote the insect’s population. In the absence of predation, assume that the population growth follows logistic model:

$$G(X) = RX \left(1 - \frac{X}{K}\right)$$

Here,  $R$  is called the growth rate and  $K$  is known as the carrying capacity of the system. Let us assume that the rate of predation follows a hill-function behaviour<sup>2</sup> as a function of the population:

$$P(X) = \frac{AX^2}{B^2 + X^2}$$

Here,  $A$  is the maximum predation rate whereas  $B$  is the half-saturation constant (because it is the population at which the predation rate is half of the maximum). Combining growth and predation together, we have a mean-field model that explains the population dynamics:

$$\frac{dX}{dt} = RX \left(1 - \frac{X}{K}\right) - \frac{AX^2}{B^2 + X^2}$$

---

<sup>2</sup>This function is called Holling type III response, with an exponent  $\theta = 2$

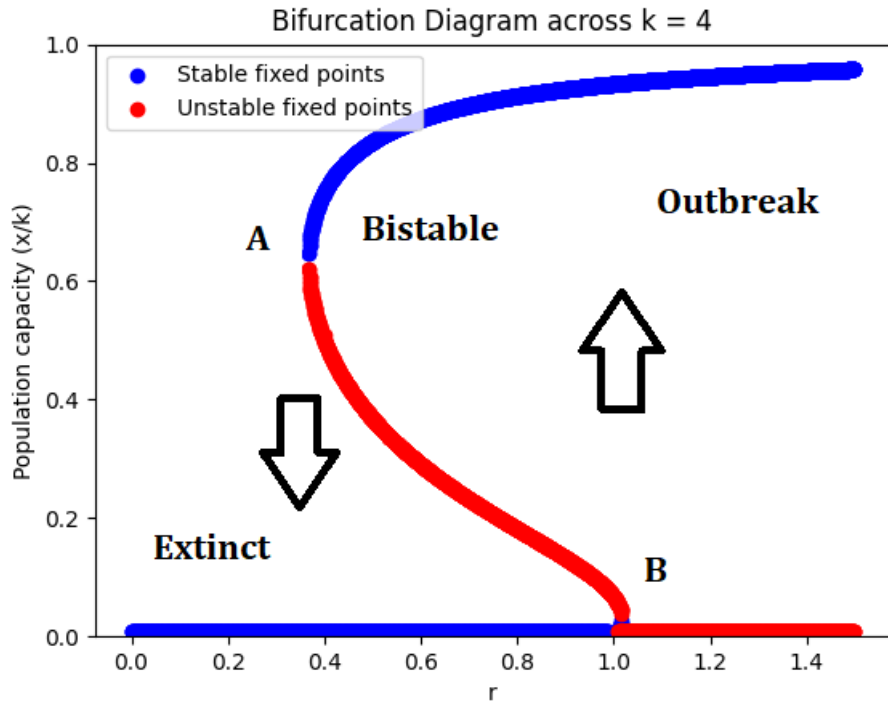


Figure 1.2: Bifurcation diagram of the harvesting/predation model

After removing redundant parameters, we have:

$$\frac{dx}{d\tau} = rx \left(1 - \frac{x}{k}\right) - \frac{x^2}{1+x^2} \quad (1.1)$$

The values of  $x$  at which the rate of change of  $x$  is 0, are called *fixed points*. A fixed point may be stable or unstable. Upon slightly nudging the population from a fixed point, if the population returns to the fixed point, then the fixed point is said to be *stable*. If the population moves away from the fixed point, then the fixed point is said to be *unstable*.

On setting the left-hand side of equation 1.1 to 0, we obtain:

$$r \left(1 - \frac{x^*}{k}\right) = \frac{x^*}{1+x^{*2}}$$

Here,  $x^*$  is used to denote the fact that the solutions of this equation are fixed points. Depending on the values of  $r$  and  $k$ , the system may have 1 stable fixed point with zero population (the extinction regime), 1 unstable fixed point between two stable fixed points (bistability regime) or 1 stable fixed point with high population (outbreak regime).

Consider the bifurcation diagram in figure 1.2. Suppose the system is at point A. If the population  $x$  or the variable  $r$  is perturbed in the lower direction, then the population will suddenly go extinct. This is an *abrupt transition*. In order to rescue the population, restoring  $r$  back to the X-coordinate of A will not suffice. One has to bring  $r$  all the way

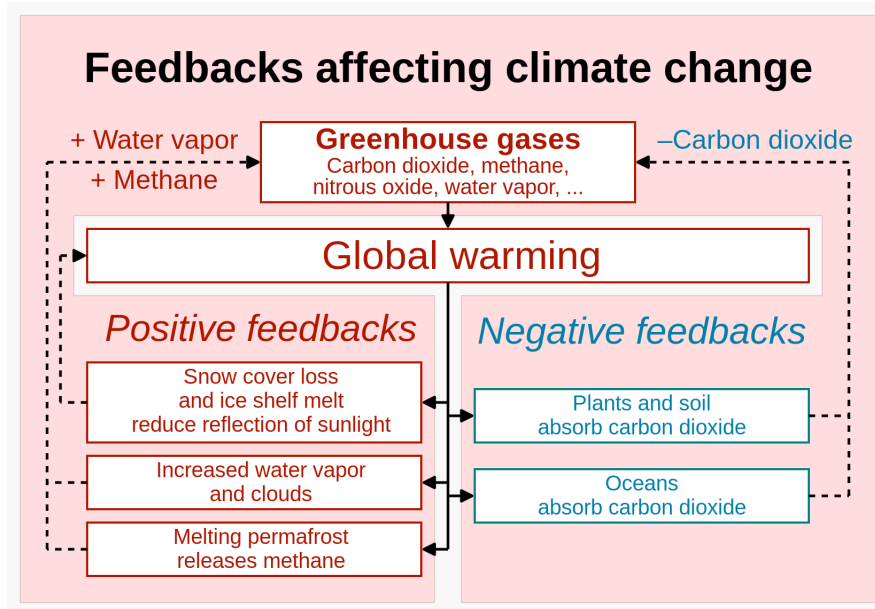


Figure 1.3: Feedback mechanisms in the global climate system

Observe how vegetation can play a role in arresting climate change. Source: [Wikimedia Commons](#)

till the X-coordinate of point B. This phenomenon, in which a system has ‘memory’ of its past, is called *hysteresis*.

This is an example of an abrupt transition in a mean-field model. Reaction-diffusion models are also known to showcase such transitions [Rietkerk et al. (2002)], as well as a phenomenon called *Turing instability* wherein the introduction of diffusion can lead to destabilization of a stable, steady state. In section 2.2, we explore a cellular automaton model that features both continuous and abrupt transitions.

Due to a variety of anthropogenic factors, ecological systems are being pushed toward critical thresholds. Abrupt transitions lead to drastic ecological disasters [Scheffer et al. (2001)]. Large ecosystems composed of various species require a delicate balance of intra-specific and inter-specific interactions in order to co-exist. The collapse of the population of a single species can have a ripple effect on the entire ecosystem. The associated fallout not only affects the local flora and fauna but also impacts the lives of people (who are most likely impoverished) whose livelihoods directly or indirectly depend on the functioning of the ecosystem.

In addition to this, the large-scale collapse of vegetation also plays a major part in the ongoing climate crisis (alongside an increase in the concentration of greenhouse gases in the atmosphere). The global climate system also features a variety of positive-feedback and negative-feedback mechanisms (refer figure 1.3). Hence, there is reason to believe that the global climate system is also prone to abrupt transitions.

## 1.3 Terminology

### 1.3.1 Cluster

A *cluster* refers to a group of connected vegetation patches in a 2D lattice. The rigorous definition of a **Von-Neumann** cluster is as follows:

- a) The Von-Neumann neighbourhood of a cell  $(i, j)$  is the set of cells:  $\{(i - 1, j), (i, j - 1), (i + 1, j), (i, j + 1)\}$ .
- b) Two cells,  $(i_1, j_1)$  and  $(i_2, j_2)$ , are called Von-Neumann neighbours if one cell belongs in the Von-Neumann neighbourhood of the other, and vice versa.
- c) A Von-Neumann path is a sequence of cells  $(i_1, j_1), (i_2, j_2), (i_3, j_3), \dots, (i_n, j_n)$  such that each consecutive pair of cells are Von-Neumann neighbours, and all cells have the same state/polarity.
- d) A set of cells  $\{(i_1, j_1), (i_2, j_2), (i_3, j_3), \dots, (i_n, j_n)\}$  belong to the same *Von-Neumann cluster* if there exists a Von-Neumann path between any two pairs of cells within the set.

Figure 1.4 serves as a visual aid in understanding Von-Neumann clusters. The same logic can be extended to obtain the concept of a *Moore cluster*. The Moore neighbourhood of a cell  $(i, j)$  is the set of cells:  $\{(i - 1, j - 1), (i - 1, j), (i - 1, j + 1), (i, j - 1), (i, j + 1), (i + 1, j - 1), (i + 1, j), (i + 1, j + 1)\}$ .

From a theoretician's perspective, since models like Tricritical Directed Percolation explicitly use Von-Neumann neighbourhood, and since percolation of agents (see 1.3.4) also happens through Von-Neumann neighbours, we prefer to stick to Von-Neumann neighbourhood. However, when working with empirical data, it is hard to discretise the landscape. The lines between Von-Neumann and Moore neighbourhoods get blurred. Additionally, these definitions are not invariant to translation and rotation of the reference frame.

### 1.3.2 Power-Law Distribution

A random variable  $X$  is said to follow a power-law distribution if its probability distribution function is given by:

$$p(x) = \alpha x^{-\beta}$$

Here,  $\alpha$  is the normalization constant, whereas  $\beta$  is known as the power-law exponent. Hence, the probability that  $X$  lies between  $x$  and  $x + dx$  is given by  $p(x)dx$ . When we

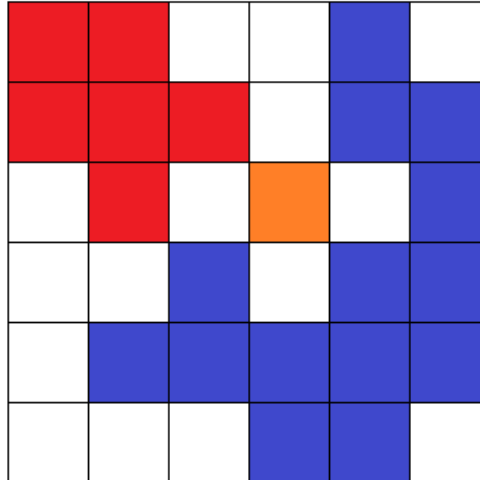


Figure 1.4: Visual aid for understanding Von-Neumann clusters  
They have been labelled using different colors

have samples of this random variable, then it is better to calculate a quantity known as complementary cumulative distribution function (or cCDF in short):

$$P(X \geq x) = \int_x^{\infty} p(x)dx = \frac{\alpha x^{-\beta+1}}{-\beta + 1}$$

The left-hand side is calculated by looking at the data. It is then plotted with respect to  $x$  on a log-log plot. According to the right-hand side, if  $X$  follows a power-law distribution, then its log-log plot must be a straight line with a negative slope.

Power-law distributions differ from other distributions in the fact that it features a fatter tail (refer figure 1.5). In fact, if  $\beta < 2$ , then the mean of the distribution is infinite since the probability density does not decay fast enough. This sort of behaviour is known as *scale invariance*. Additionally, the variance is infinite if  $\beta < 3$ .

Power-law distributions arise when certain positive feedback mechanisms are in place. Phase transitions in certain systems are also signalled by the emergence of power-law distribution in certain quantities. Hence, it is no surprise that the vegetation patch sizes in semi-arid ecosystems are known to follow a power-law distribution.

### 1.3.3 Cellular Automaton

A cellular automaton consists of a regular N-dimensional lattice of cells. Each cell can be in a finite number of states. The concept of a neighbourhood should be defined. The future state of a given cell is determined according to a set of rules and is contingent on the states of the neighbouring cells. This process may be deterministic or probabilistic. The cells may be asynchronously or synchronously updated.

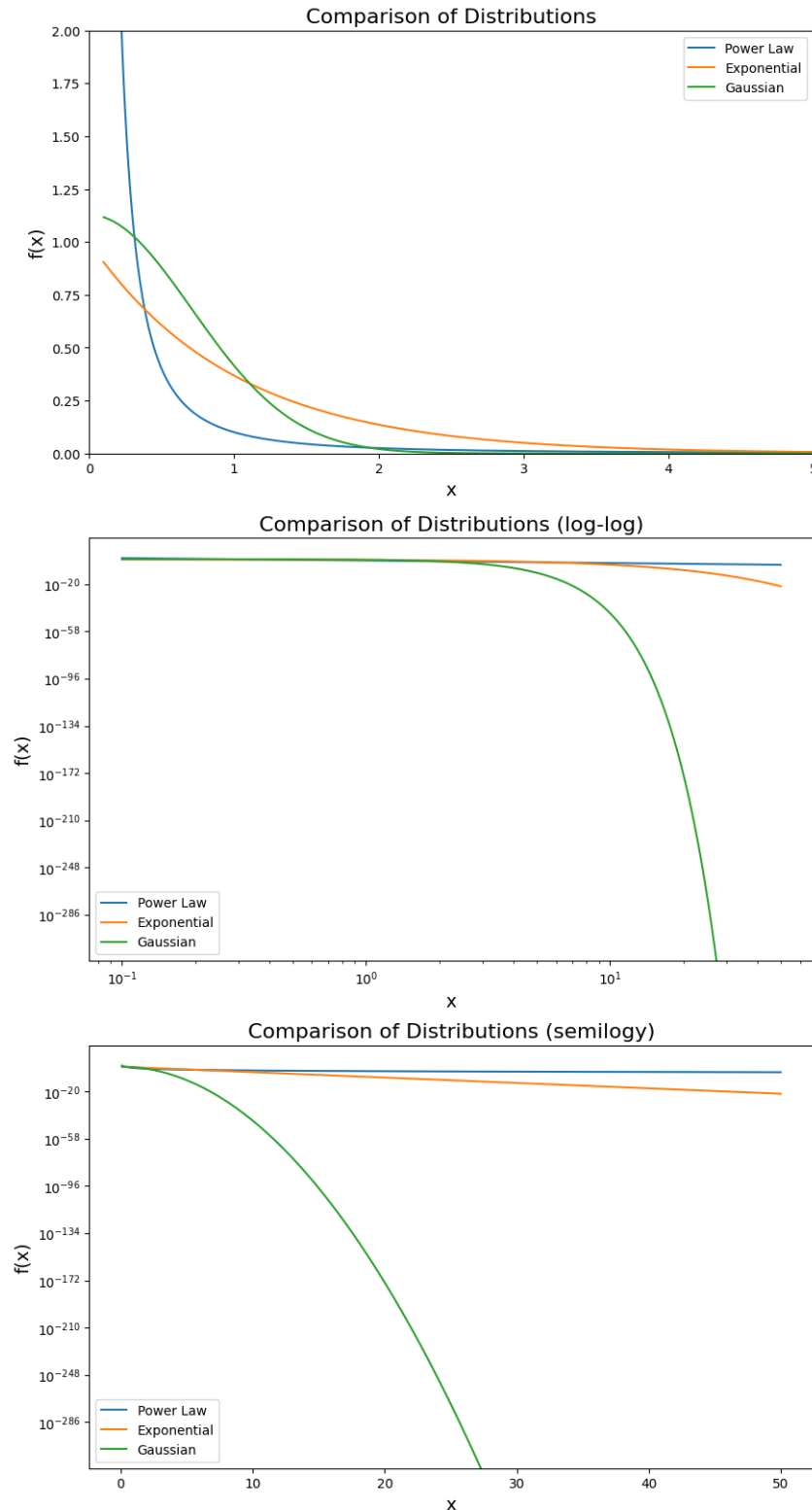


Figure 1.5: Comparison of normalized power-law ( $x^{-\beta}$ ), exponential ( $e^{-x}$ ) and Gaussian ( $e^{-x^2}$ ) distributions

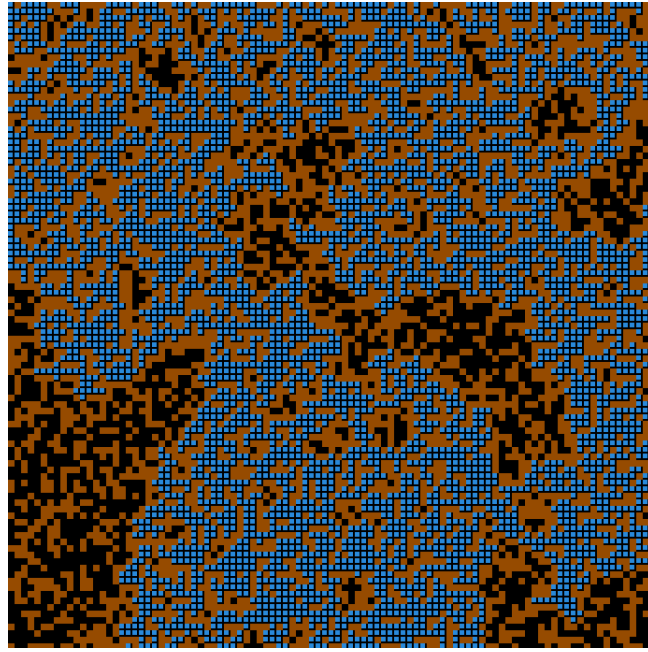


Figure 1.6: Depiction of a percolating cluster

In this figure, the mobile agent (blue) has *percolated* through the porous media consisting of solid (green) and vacant (black) sites

An example of a deterministic, synchronously-updated cellular automaton is Conway's Game of Life ([interactive simulation here](#)) Although this cellular automaton is based on a simple set of rules, it is possible to build self-replication machines and Turing-complete computers within this system. All models used in this thesis are examples of probabilistic cellular automata.

### 1.3.4 Percolation

Consider a two-dimensional lattice of cells such that the state of each cell can be either 0 or 1. The lattice may be randomly generated (keeping some fractional occupancy in mind), or it may be the final result of a model.

The lattice is said to feature a *percolating cluster* (figure 1.6) if there exists a single cluster that spans the entirety of the lattice. The density at which a percolating cluster is most certainly present is called *percolation density*.

In randomly generated lattices, a percolating cluster is most certainly present when the fractional occupancy is above 0.59. This phenomenon is called site percolation ([interactive simulation here](#)). Models may increase or decrease this figure depending on their behaviour. The parameter of a model above which a percolating cluster is most certainly present is called *percolation threshold*.

## 1.4 Early Warning Signals in Literature

Systems that are approaching critical thresholds are known to showcase certain behaviours [Kéfi et al. (2014)]. These behaviours are called *early warning signals* in literature. Early warning signals not only herald imminent transitions but may also convey information about the type of transition and the closeness of the threshold. Observation of early warning signals can equip us to take steps towards restoration of the ecosystems and thereby prevent ecological disasters and the associated economic losses. Here, we review some early warning signals for patchy ecosystems that have already been studied in literature:

### 1.4.1 Cluster Size Distribution

[Scanlon et al. (2007)] devised a probabilistic cellular automaton for semi-arid ecosystems. The cluster size distribution generated by this model was similar to that obtained from empirical data in the Kalahari transect. The authors of the paper speculated whether semi-arid ecosystems exhibit *self-organized criticality*: the tendency of a system to evolve towards critical points. They postulated that its scale-invariant features near critical points might contribute to the robustness of the system.

[Kéfi et al. (2007a)] used empirical data from semi-arid vegetation in the Mediterranean. They measured grazing pressure via GPS-tracking of sheep. They observed that a higher grazing pressure is accompanied by a deviation of cluster sizes from a power-law distribution. They also proposed a model that replicated the same result.

However, [Sankaran et al. (2019)] used a directed percolation model to show that when positive feedback is high enough, then power-law clustering is observed even at the critical threshold. Hence, deviation of cluster sizes from a power-law distribution is not a reliable indicator of approaching thresholds. Instead, they proposed another indicator (see 1.4.3). On the flip side, [Weissmann and Shnerb (2014)] advocated for study of void size distributions in certain regimes.

### 1.4.2 Cluster Growth Probabilities

[Weissmann and Shnerb (2016)] simulated two models (one model featuring an abrupt transition, whereas the other model had a continuous transition) and tracked individual clusters for growth and decay (in a very coarse-grained manner). Based on the generated data, for a given cluster size, they computed the probability with which it will grow or decay. If the probability of growth increases with cluster size, then the system involves positive feedback mechanisms. Hence, the system features an abrupt transition, and vice

versa.

The cluster size which has equal probability of growing and decaying is called *critical cluster size*. If a system features abrupt transitions, then an increase in the critical cluster size indicates that the system is nearing the critical threshold. On the other hand, if a system features a continuous transition, then a decrease in the critical cluster size indicates that the system is nearing the critical point.

### 1.4.3 Spatial Autocovariance

The theory of phase transitions postulates that some features of a system become scale-free as and when the system approaches a phase transition. [Sankaran et al. (2019)] claims that this feature (for models of semi-arid vegetation) is the *spatial autocovariance function*. They simulated a directed percolation model and computed the spatial autocovariance function by performing an inverse Fourier transform of the power-spectrum of the final lattice (refer *Wiener Khinchin theorem*). They observed that the power spectrum indeed decays as a power-law function of the spatial frequency.

[Majumder et al. (2019)] also utilized spatial metrics like spatial variance and spatial autocorrelation to infer critical thresholds, and applied it on empirical data.

### 1.4.4 Critical Slowing Down

This is a generic indicator of approaching critical thresholds. Consider a dynamical system described by the following equation:

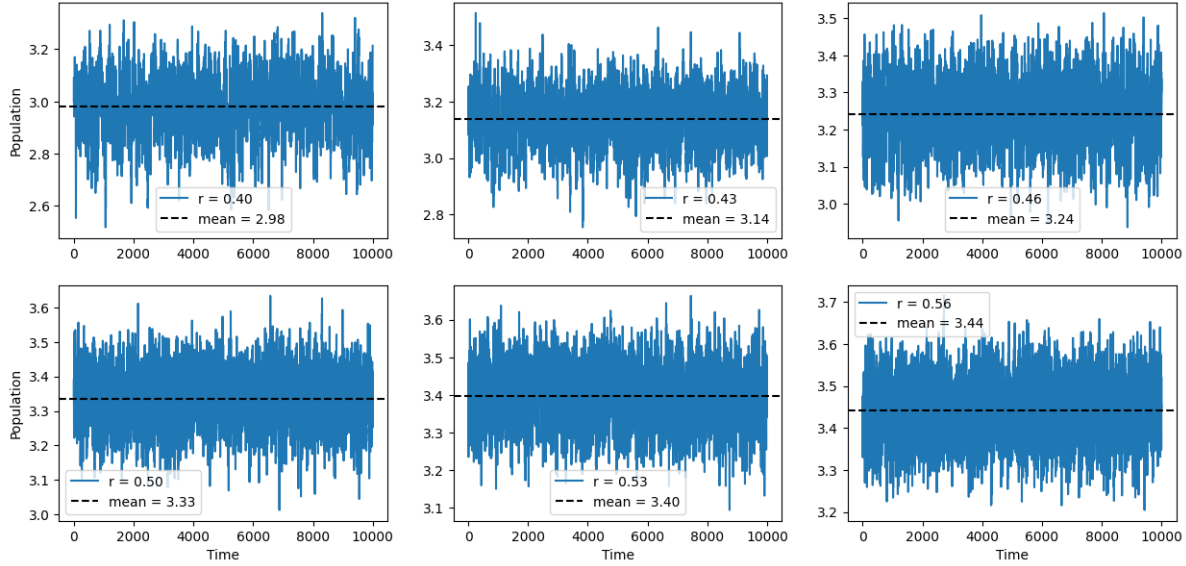
$$\dot{x} = f(x)$$

where  $x$  can be a single variable or a vector. The *landscape potential* associated with the dynamical system is defined as follows:

$$U(x) = - \int_{x_0}^x f(x') dx'$$

At fixed points  $x^*$  of the system, the landscape potential is flat ( $U'(x^*) = 0$ ). If a fixed point is stable, then it lies at the bottom of a well. Similarly, if a fixed point is unstable, then it lies at the top of a hill. The effect of perturbing the system is analogous to the behaviour of a perturbed ball that is initially located at these points.

As the system approaches a critical threshold, the potential well in which a stable, fixed point is located begins to get ‘shallower’ and ‘wider’. If the system is perturbed from this state, then it takes longer to return to the fixed point. When we analyse

Figure 1.7: Population time series for different values of  $r$ 

the time-series data of such a system, we observe oscillatory behaviour around the fixed point. This translates to *higher variance* around the fixed point. If the potential well is asymmetric around the fixed point, then the system spends more time in the shallower section of the well and less time in the steeper section of the well. In time-series data, this translates to *higher skewness* around the fixed point [Guttal and Jayaprakash (2008)].

On account of being close to a critical threshold, the phenomenon due to which a system spends more time oscillating around its fixed point is called *critical slowing down*. The sign of  $f(x^*)$  tells us if the fixed point  $x^*$  is stable or not.  $f(x^*) < 0$  implies that the fixed point is stable, and vice versa. On the other hand,  $\frac{1}{|f(x^*)|}$  is called *return time*: it is proportional to the time that the system takes to return to its stable fixed point after being perturbed. As a system approaches its critical threshold,  $f(x^*) \rightarrow 0 \implies$  *return time*  $\rightarrow \infty$ . In essence, the system takes forever to return to its stable fixed point. This is the reason why the phenomenon in question is called critical *slowing down*.

Let us demonstrate critical slowing down in the harvesting/predation model presented in section 1.2. Consider figure 1.2. An abrupt transition occurs around  $r = 0.38$ . We simulate this model at different values of  $r$  near this threshold, accompanied with the same amplitude of Gaussian noise (figure 1.7). Observe how the variance increases as the system is stressed (figure 1.8). This is because the system takes a longer time to return to its fixed point.

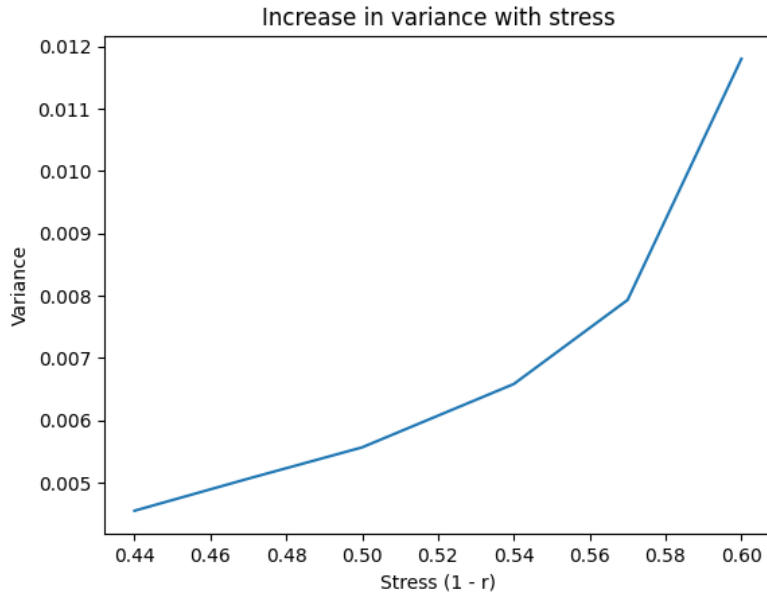


Figure 1.8: Increase in variance due to critical slowing down

## 1.5 Objectives

In section 1.1, we identified our systems of interest: patchy ecosystems. Why are we interested in these? Not only do these systems span considerable swathes of the world, but they are also poised to collapse due to a variety of factors. Additionally, we have high-resolution satellite data of semi-arid vegetation over a temporal range - data that can be used to test our findings.

In section 1.2, we established different modelling techniques for dynamical systems. We claimed that all these models feature transitions. We laid down the concept of fixed points and their stability, as well as presented a harvesting/predation model to showcase abrupt transitions and hysteresis. We cautioned that the collapse of ecosystems can have disastrous consequences for plants, animals, and humans alike. This is why theoretical ecologists come up with early warning signals that forewarn the approach of critical thresholds.

In section 1.4, we enumerated different early warning signals that are already presented in literature. The aim of this work is to add another technique to this arsenal; techniques that are yet to be explored.

### Aims

- To deduce whether the distribution of change of cluster sizes contains information about approaching thresholds, and can therefore be used as an early warning signal.
- To analyze the cluster dynamics as a function of cluster size, and thereby formulate

a stochastic mean field model for cluster sizes.

## Contributions

- Developed programs that simulated 3 models of patchy ecosystems (contact process, tricritical directed percolation and Scanlon's model) and studied their phase transitions and percolation properties.
- Also simulated 2 null models to serve as control for cluster distribution and cluster dynamics.
- Formulated and implemented a cluster tracking algorithm to calculate the quantity of interest from time series data of lattices.
- Analysed the cluster size distribution and cluster dynamics of TDP model, and devised a stochastic mean field approximation of it.

## Results

Identified three behaviours (of which two are novel) that can serve as early warning signals for an impending critical transition in patchy ecosystems:

- a) Deviation of cluster size distribution from power-law behaviour
- b) Exponential behaviour of cluster dynamics
- c) Rapid decay in critical cluster size

## Organization of this thesis

This is how the thesis is organized: in chapter 2, we explain the working of the models we use, as well as description of their features. In chapter 3, we describe the cluster tracking algorithm that allows us to generate the quantity we are interested in. We also explain a statistically rigorous way of evaluating goodness of power-law fits. Chapter 4 contains all the results generated using TDP model. They are also compared with results from the null model. Finally, in chapter 5, we interpret trends in the results and formulate early warning signals.

# Chapter 2

## Models

### 2.1 Contact Process

This model consists of a two-dimensional lattice of cells. Each cell can be in a discrete number of states, namely: 0 (unoccupied) or 1 (occupied by vegetation). This model is completely described by only one parameter,  $p$ , which is a number between 0 and 1 because it represents a probability. An interactive simulation of this model can be found [here](#).

#### 2.1.1 Working of the model

- 1) Select a cell at random
- 2) If it is unoccupied, then return to step 1. Otherwise, proceed to the next step
- 3) With probability  $p$ , randomly choose a cell in the Von-Neumann neighbourhood of the selected cell. If the chosen cell is empty, then update the state of the cell from 0 to 1. If the chosen cell is occupied then do nothing
- 4) Otherwise (with probability  $1 - p$ ), update the state of the selected cell from 1 to 0
- 5) Return to the first step

To be more rigorous, contact process is a stochastic process that describes population growth on an interconnected graph. Occupied sites become empty at a constant rate, whereas empty sites become occupied at a rate proportional to the number of neighbouring occupied sites.

The next model is an extension of this model. Hence, the phase transitions and percolation transitions of this model are featured in the next section.

## 2.2 Tricritical Directed Percolation

This model revolves around a two-dimensional lattice of cells. Each cell can be in a discrete number of states, namely: 0 (unoccupied) or 1 (occupied by vegetation). The model features only two parameters:  $p$  and  $q$ . Both numbers are between 0 and 1 because they represent probabilities. This model is an extension of the Contact Process model. In fact, when  $q = 0$ , this model behaves akin to the previous model. An interactive simulation of this model can be found [here](#).

### 2.2.1 Working of the model

- 1) Select a cell at random
- 2) If it is unoccupied, then return to step 1. Otherwise, proceed to the next step
- 3) The selected cell (henceforth referred to as the ‘focal cell’) has four Von-Neumann neighbours. Select one of these four neighbours at random. If the selected neighbour cell is unoccupied, then proceed to step 4. Otherwise, skip to step 5
- 4) With probability  $p$ , update the state of the selected neighbour cell from 0 to 1. Otherwise (with probability  $1 - p$ ), update the state of the focal cell from 1 to 0. Return to the first step (this step is identical to contact process).
- 5) The focal cell and the selected neighbour cell together have 6 neighbours. Select one neighbour at random. With probability  $q$ , make sure that the state of this cell is 1 (irrespective of its initial state). Otherwise, with an overall probability of  $(1-p)(1-q)$ , update the state of the focal cell from 1 to 0. Return to the first step

### 2.2.2 Transition Probabilities

- a) The transition in the first half of step 4 is called *stochastic birth*. It happens with probability  $p$ :

$$10 \rightarrow 11$$

- b) The transition in the second half of step 4 is called *stochastic death*. It happens with probability  $1 - p$ :

$$10 \rightarrow 00$$

- c) The transition in the first half of step 5 is called *positive feedback birth*. This transition provides an additional mode of birth. It happens with probability  $q$ :

$$110 \rightarrow 111$$

- d) The transition in the second half of step 6 is called *density death*. This transition provides an additional mode of death. However, note that the probability of death has been reduced from  $1 - p$  (as in transition b) to  $(1 - p)(1 - q)$ :

$$11 \rightarrow 10$$

Based on how  $p$  and  $q$  affect the rates of these transitions,  $p$  is called *baseline birth probability* whereas  $q$  is called *positive feedback*. Since the above transitions have corresponding analogies in the interactions of patchy ecosystems, this percolation model has piqued our interest. To be more specific,  $p$  is the baseline birth probability (or  $1 - p$  acts as stress) that acts globally, whereas  $q$  denotes the extent of facilitation.

All possible transitions in this model, as well as their probabilities, have been depicted in figure 2.1.

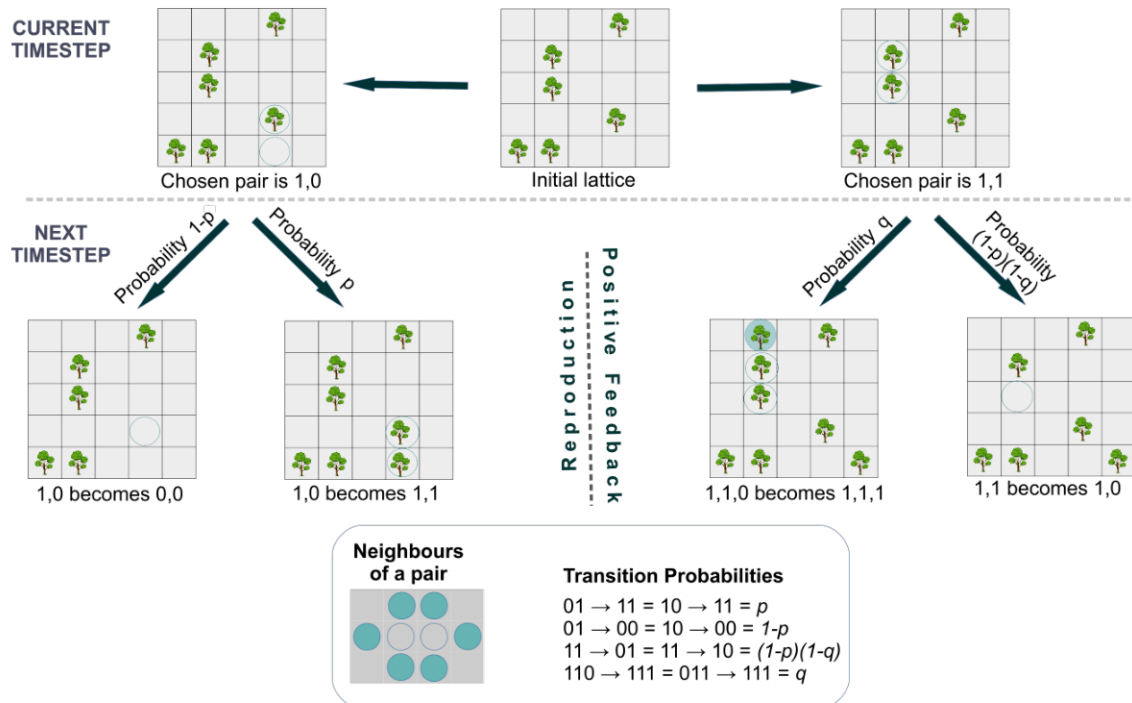


Figure 2.1: Schematic of TDP model  
This image has been taken from [Sankaran et al. (2019)]

### 2.2.3 Phase Transitions

The state variable of this model is the *fractional occupancy*  $\rho$ : the fraction of cells that are occupied. To gain an insight into the working of this model, we look at the relationship between  $\rho$  and  $p$ . We also observe how this relationship varies with the value of  $q$ .

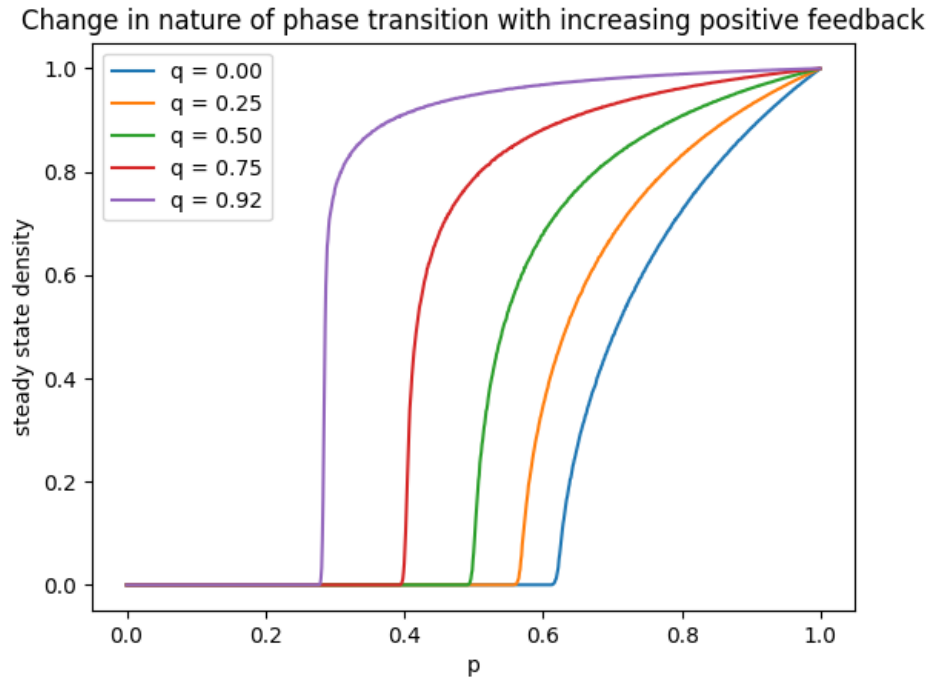


Figure 2.2: Behaviour of TDP model for various values of  $q$

At  $q = 0$ ,  $\rho$  is 0 until  $p = 0.62$ . The birth probability isn't high enough to sustain a population. As  $p$  increases beyond 0.62,  $\rho$  slowly rises. This phase transition is hence *continuous*. At  $q = 0.92$ ,  $\rho$  is 0 until  $p = 0.28$ . However, as  $p$  increases beyond 0.28,  $\rho$  abruptly rises. For example: at  $p = 0.29$ ,  $\rho = 0.69$ . This phase transition is hence *abrupt*. Both these transitions are depicted in 2.2, alongside other values of  $q$ .

This model's remarkable feature is that not only is it entirely characterized by just two numbers:  $p$  and  $q$  (both numbers between 0 and 1), but it also features both continuous and abrupt transitions. Since ecosystems are known to involve both types of transitions, the results from this model are ubiquitous. The overall behaviour of this model is conveyed by the phase diagram in figure 2.3

## 2.2.4 Percolation Transitions

For a given value of  $q$ , the percolation threshold  $p_p$  is the value of  $p$  at which there is a non-zero probability that a percolation cluster is present. The percolation density  $\rho_p$  is the density corresponding to the value of  $(p_p, q)$ . It is noticed that as positive feedback ( $q$ ) increases, the value of  $p_f$  as well as  $\rho_f$  decreases. Figure 2.4 depicts the percolation thresholds whereas figure 2.5 showcases the percolation transitions.

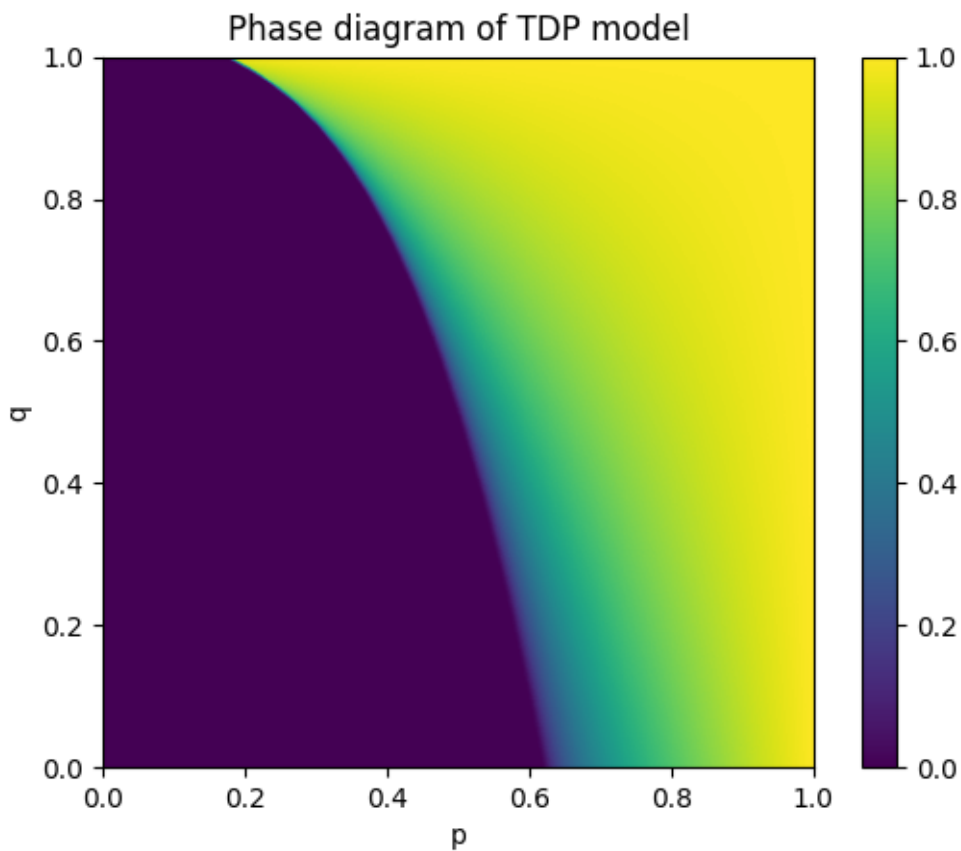


Figure 2.3: Phase diagram of TDP model

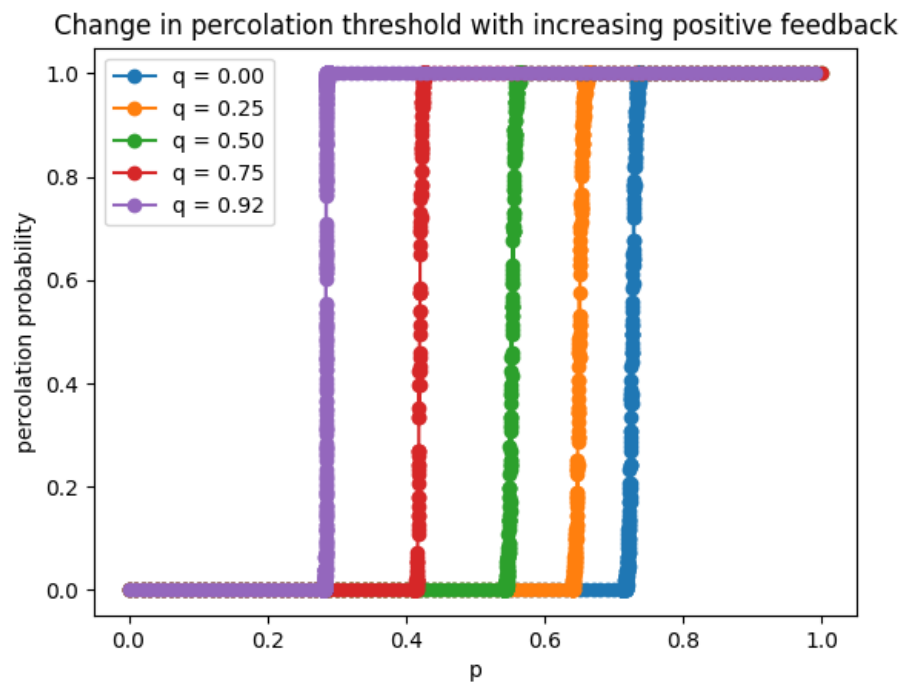


Figure 2.4: Percolation thresholds of TDP model

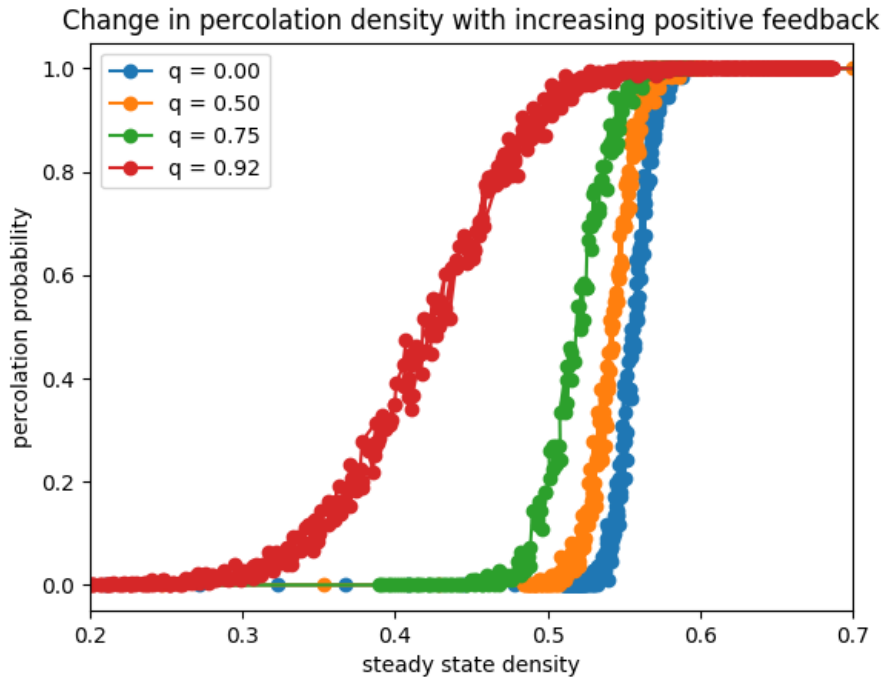


Figure 2.5: Percolation transitions of TDP model

## 2.3 Scanlon's Model

This model was formulated in [Scanlon et al. (2007)]. Just like Tricritical Directed Percolation, this model is composed of a two-dimensional lattice of cells. Each cell can be in a discrete number of states: namely 0 (unoccupied) or 1. However, this model features an extended set of weakly-bounded parameters: rainfall (the primary parameter), the radius of influence, and immediacy.

### 2.3.1 Working of the model

Select a random cell  $(i, j)$  (the cell in the  $i^{th}$  row and  $j^{th}$  column). Based on its initial state, transition it to the alternate state with the following probabilities:

$$P_{ij}(0 \rightarrow 1) = \rho_{ij} + \frac{f^* - f_t}{1 - f_t} \quad (2.1)$$

$$P_{ij}(1 \rightarrow 0) = (1 - \rho_{ij}) + \frac{f_t - f^*}{f_t} \quad (2.2)$$

$$\text{where } \rho_{ij} = \frac{\sum_{(a,b) \in C_{ij,r}} \left(1 - \frac{d_{ij,ab}}{k}\right) x_{ab}}{\sum_{(a,b) \in C_{ij,r}} \left(1 - \frac{d_{ij,ab}}{k}\right)} \quad (2.3)$$

$f_t$  is the current fractional cover.  $f^*$  is the fractional cover supported by the region, based on the rainfall (in mm/year) it receives. [Scanlon et al. (2007)] obtained the following linear relationship by utilizing empirical data of semi-arid vegetation in the Kalahari transect:

$$f^* = 0.0008588 * (\text{rainfall}) - 0.1702 \quad (2.4)$$

Additionally,  $f^*$  is constrained to be between 0 and 1.

$C_{ij,r}$  is the set of cells lying within a distance  $r$  of the  $(i,j)$  cell.  $r$  is the radius of influence.  $d_{ij,ab}$  is the distance between the  $(i,j)$  cell and the  $(a,b)$  cell.  $x_{ab}$  is the state of the  $(a,b)$  cell (either 0 or 1).  $k$  is a quantity known as *immediacy*. It quantifies the additional weightage given to closer cells.

The second term in both equations 2.1 and 2.2 make the model's fractional cover  $f_t$  approach the intended fractional cover  $f^*$ . Equation 2.3 denotes the positive feedback.  $\rho_{ij}$  is a value between 0 and 1. If all cells in the neighbourhood of the  $(i,j)$  cell (that is, all cells within radius  $r$ ) are fully occupied, then  $\rho_{ij} = 1$ , and vice versa. This term promotes birth and inhibits death. It is responsible for producing patchy vegetation.

Simulations show that the fractional cover varies linearly with rainfall, as dictated by equation 2.4. Hence the phase/bifurcation diagram is simple (figure 2.6).

### 2.3.2 Percolation Transitions

Since the density of this model linearly increases with rainfall, one can obtain percolation transitions from percolation thresholds. Hence, only percolation thresholds are discussed.

When immediacy is kept constant (figure 2.7), it is observed that percolation threshold increases with radius of influence. Additionally, the transition is more abrupt for higher radius of influence.

When radius of influence is kept constant (figure 2.8), no conclusive trend is observed with changing immediacy. This leads us to speculate that immediacy is not an important parameter. In fact, [Manor and Shnerb (2008)] got rid of immediacy and assigned equal weightage to all cells within the radius of influence.

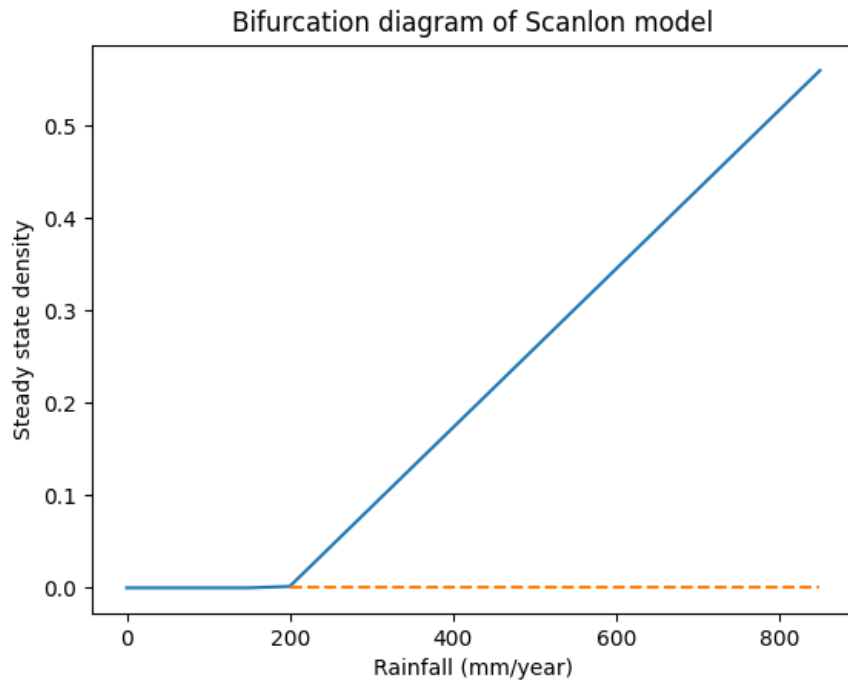


Figure 2.6: Bifurcation diagram of Scanlon's model

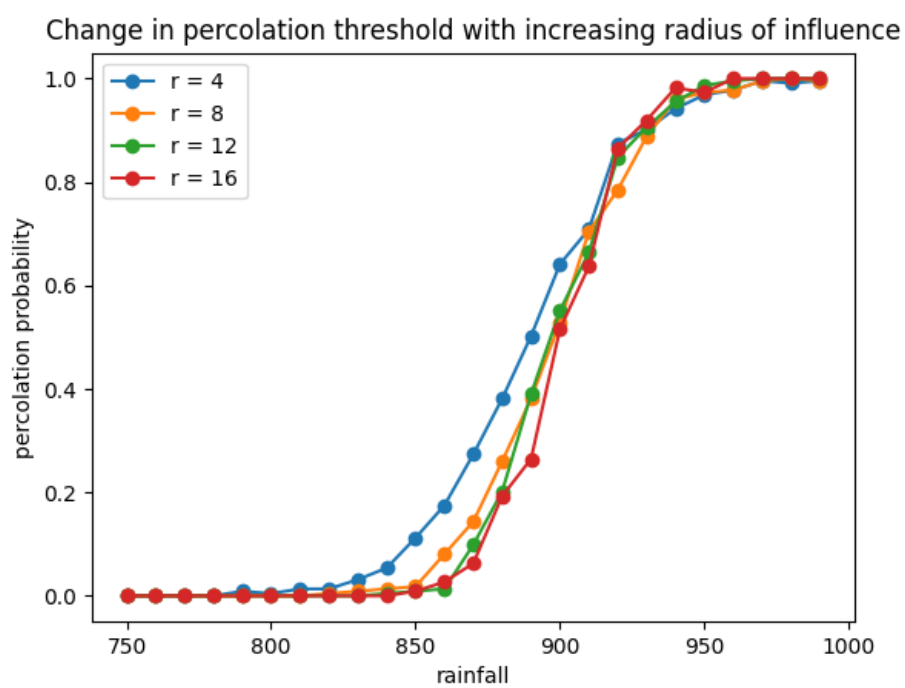


Figure 2.7: Variation of percolation threshold with increasing radius of influence in Scanlon's model

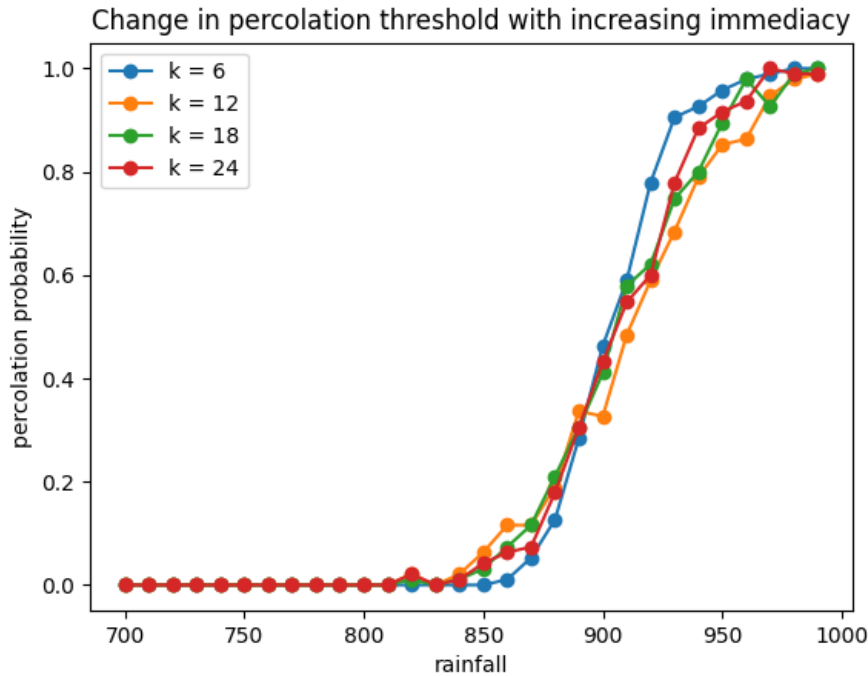


Figure 2.8: Variation of percolation threshold with increasing immediacy in Scanlon’s model

## 2.4 Null Model for Cluster Size Distribution

We require a null model to serve as a control for cluster size distribution. It must randomly populate a binary lattice according to a given fractional occupancy  $f$ .

### 2.4.1 Percolation Transitions

As already stated in section 1.3.4, this model undergoes a percolation transition at a density of 0.59 (figure 2.9)

## 2.5 Null Model for Cluster Dynamics

We require a null model to serve as a control for cluster dynamics. This model should not only produce completely random landscapes but also evolve in a completely random manner. We utilized the null model proposed in [Kéfi et al. (2011)]. Let  $f$  be the fractional occupancy of the landscape. Let  $r$  be the rate at which empty cells get colonized, and  $m$  be the rate at which occupied cells become empty, then the dynamics of the system is given by:

$$\frac{df}{dt} = r - (m + r)f$$

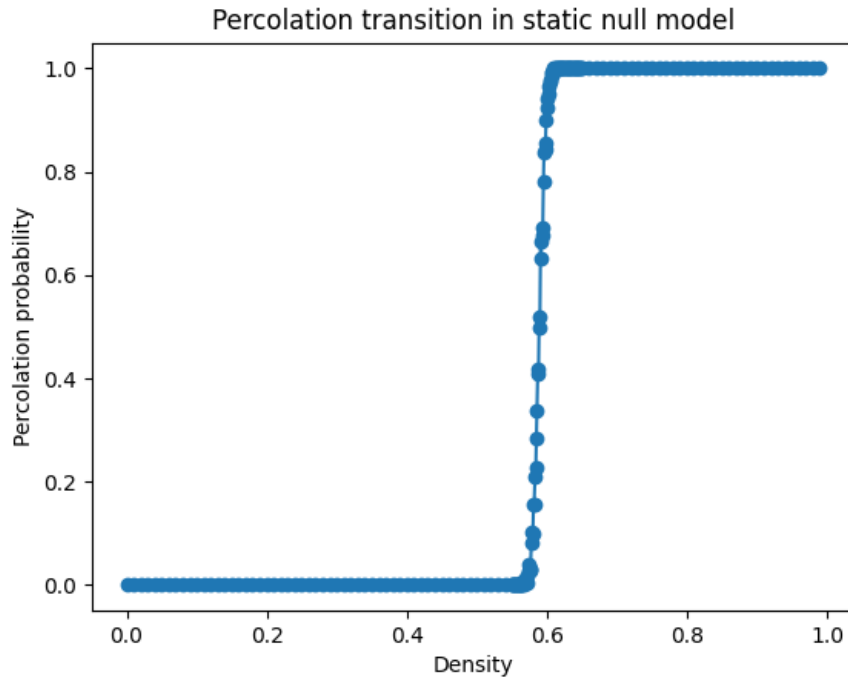


Figure 2.9: Percolation transition in static null model

This equation has a fixed point at  $f^* = \frac{1}{1+(m/r)}$ . Hence, we choose  $m$  and  $r$  such that we obtain the intended fractional occupancy. The rates are converted to probabilities using the Gillespie algorithm.

### 2.5.1 Percolation Transitions

Since this model is initialized with a required occupancy in mind, its percolation transitions should not differ from that of the static null model. That is indeed the case (figure 2.10). However, we must also note that the update rules of this model have not affected its percolation characteristics. Hence, the dynamics of this model is truly *random*.

## Disclaimer about the phase transitions and percolation thresholds in this thesis

Please note that the analysis of phase transitions done here is not similar to what physicists do. We merely simulated the model(s) across a range of parameters values in order to deduce the critical points as well as the type of transitions. We are not interested in carrying out an Ehrenfest classification, nor are we interested in order parameters and universality classes.

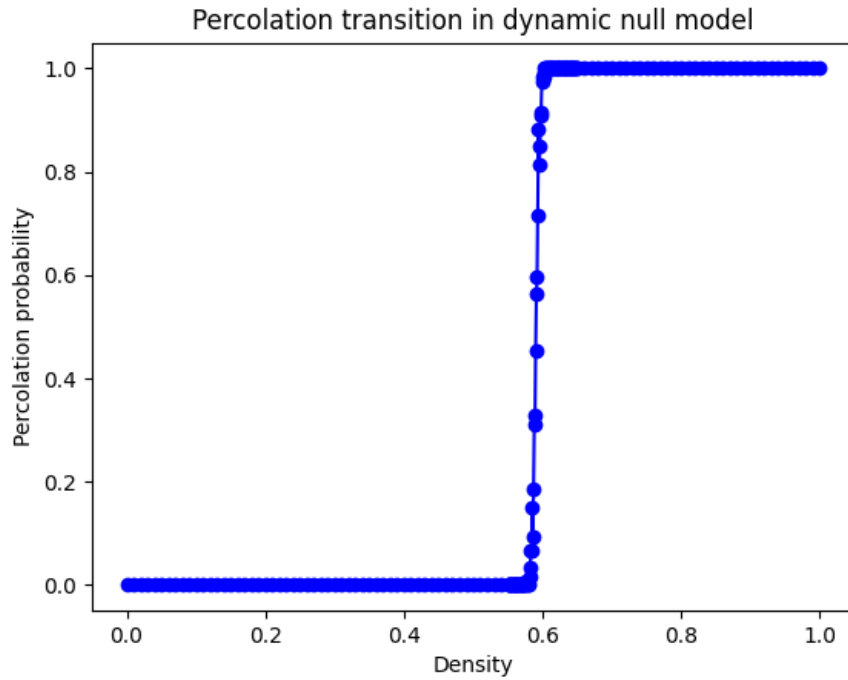


Figure 2.10: Percolation transition in dynamic null model

In a similar vein, a rigorous analysis of percolation not only requires running thousands of ensembles of the model with larger spatial extent, but also entails a procedure called *finite size scaling*. The latter allows us to deduce properties of the model when the system size is infinite.

In this work, we studied the percolation behaviour of models in order to approximate their percolation thresholds. We wanted to see how the dynamics of our models change across percolation thresholds. Calculating critical exponents is not the goal of this thesis, hence we did not perform the aforementioned rigorous analysis.

# Chapter 3

## Methods

### 3.1 Cluster Tracking Algorithm

When given an old lattice and a new lattice that has undergone only one update, we need a program that identifies the following:

- The process that the lattice underwent, and the sizes of the participating clusters
- The change in cluster size associated with the process. When multiple clusters are involved, we consider the biggest participating cluster as our reference

This program first identifies the cluster(s) that have undergone change(s). Then, it looks at the size(s) of the changing cluster(s) to come up with the aforementioned information.

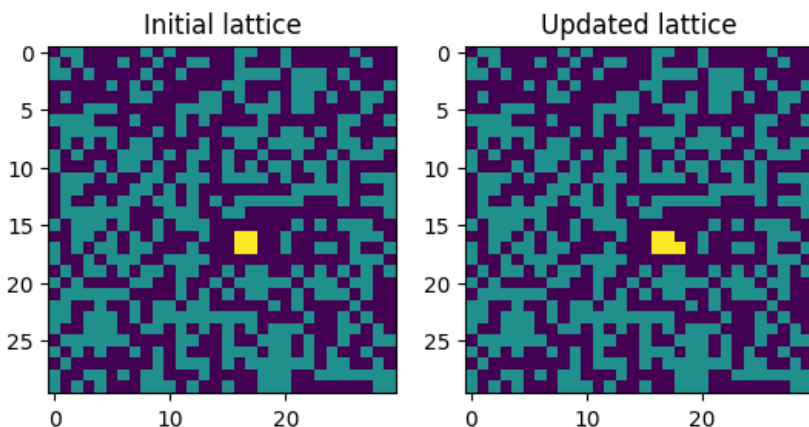
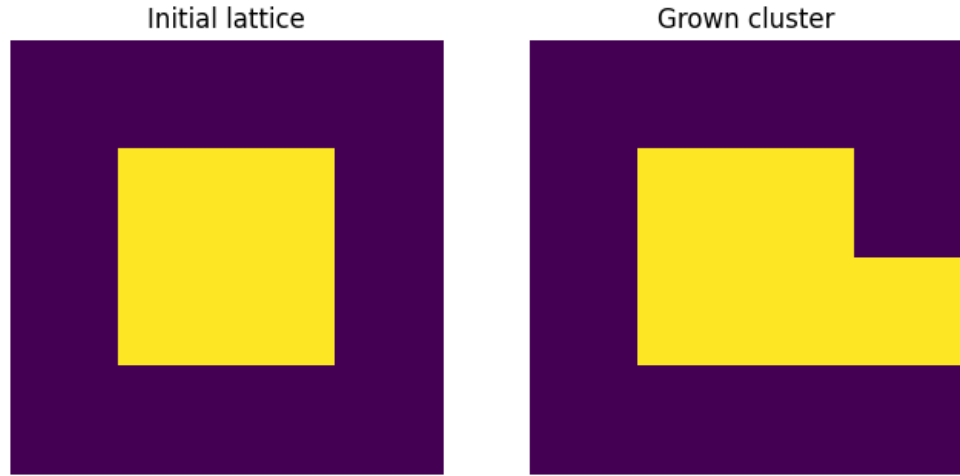


Figure 3.1: An example of two lattices that differ by only one update

Here, we show the working of our cluster tracking algorithm on small ( $4 \times 4$ ) lattices.

## Growth

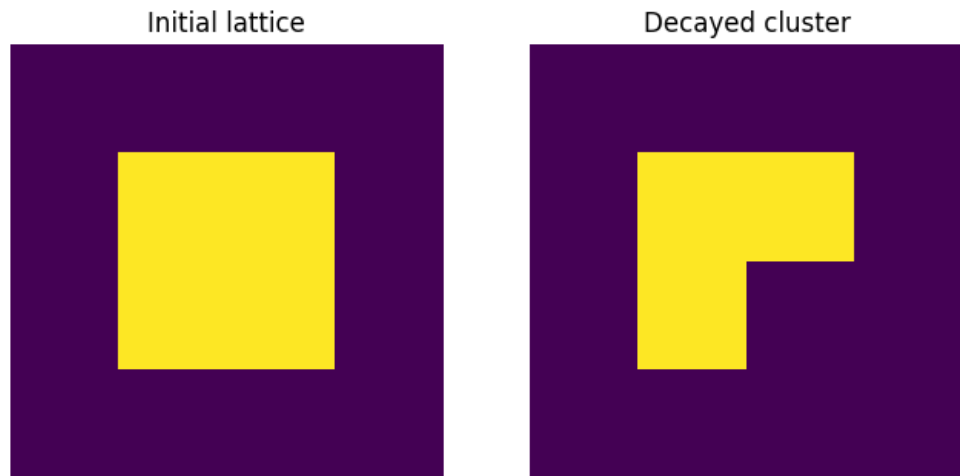


**Program output:** `{'type': 'growth', 'size': 4}`

**Interpretation:** A cluster of size 4 has grown (to size 5)

**Change:** +1

## Decay

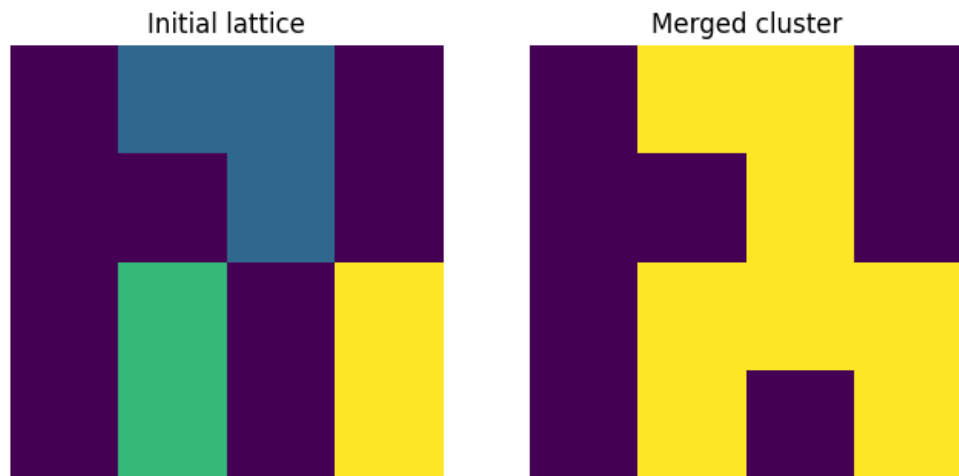


**Program output:** `{'type': 'decay', 'size': 4}`

**Interpretation:** A cluster of size 4 has decayed (to size 3)

**Change:** -1

## Merge

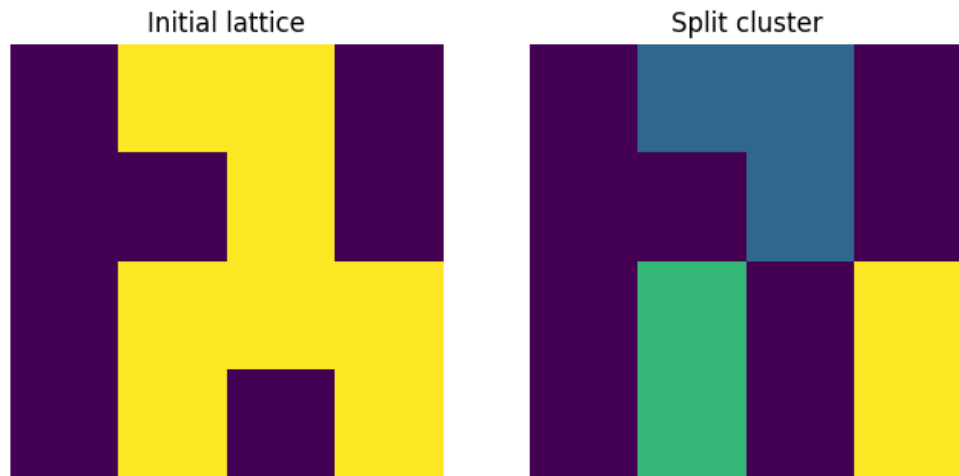


**Program output:** `{'type': 'merge', 'initial_sizes': [3, 2, 2], 'final_size': 8}`

**Interpretation:** Clusters of sizes 3, 2, 2 merged to form a cluster of size 8

**Change:**  $8 - \max(3, 2, 2) = +5$

## Split

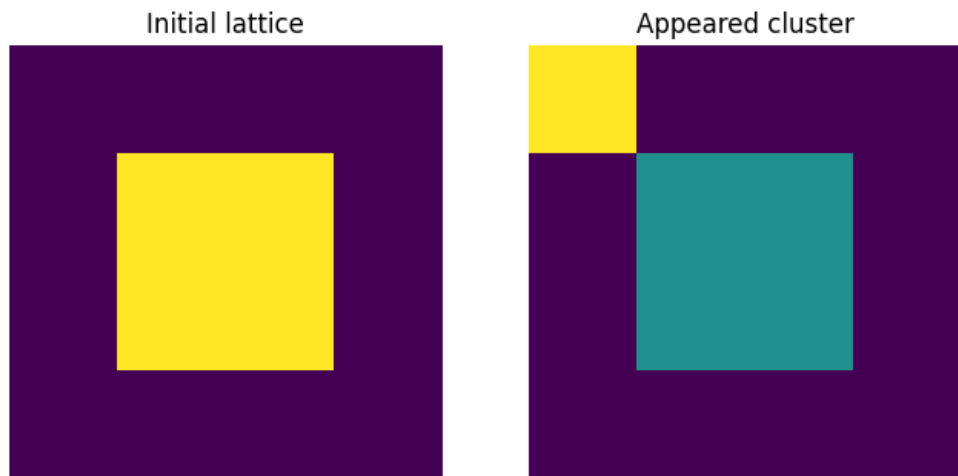


**Program output:** `{'type': 'split', 'initial_size': 8, 'final_size': [3, 2, 2]}`

**Interpretation:** A cluster of size 8 split into clusters of sizes 3, 2, 2

**Change:**  $\max(3, 2, 2) - 8 = -5$

## Appearance

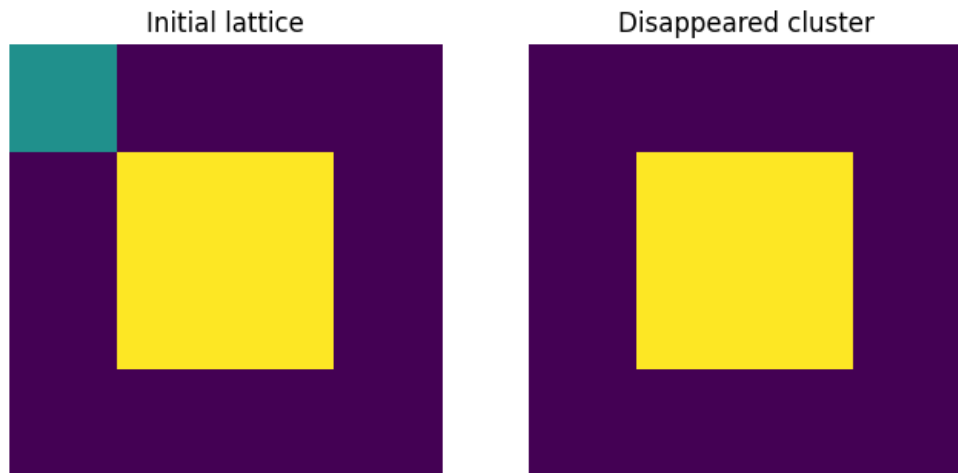


**Program output:** {type: 'appearance'}

**Interpretation:** A cluster (of size 1) appeared

**Change:** +1

## Disappearance



**Program output:** {type: 'disappearance'}

**Interpretation:** A cluster (of size 1) disappeared

**Change:** +1

## 3.2 Evaluation of Goodness of Power-law Fits

When fitting a given sample to a power-law distribution, one must realize that the points in the heavy-tailed regions are relatively more important. Given a distribution, Maximum Likelihood Estimation (MLE) is a method of estimating the parameters of said distribution. It is achieved by maximizing a likelihood function using optimization methods like gradient descent or BFGS.

A sample that shows power-law behavior can potentially be fit to an exponential distribution as well:

$$f(x) = A \exp(-bx)$$

Some quantities have been observed to follow power-law distribution up to a certain point  $x_c$ , after which they show an exponential decay. Such a distribution is called power law with an exponential cutoff (PLE) or a truncated power-law (TPL):

$$f(x) = Ax^{-\beta} \exp\left(-\frac{x}{x_c}\right)$$

Given a sample, how do we determine which distribution is the best fit? [Clauset et al. (2009)] tackles this problem in detail, and advocates the usage of a quantity called Bayesian Information Criteria (BIC):

$$BIC = k \ln n - 2 \ln \hat{\mathcal{L}} \tag{3.1}$$

where  $k$  is the number of parameters featured in distribution being fit,  $n$  is the number of samples in the given data, and  $\hat{\mathcal{L}}$  is the maximum value of the likelihood function. The distribution which has a lower value of BIC is the best fit. We utilize the R package described in [Génin et al. (2018)] to calculate the log-likelihood and calculate BIC using equation 3.1. We do this process for cluster size distribution as well as the changes in cluster sizes.

### 3.3 Process of SDE Discovery

The stochastic dynamics of a quantity  $x$  can be modeled using the following equation:

$$\dot{x} = f(x) + g(x)\eta(t) \quad (3.2)$$

here,  $f(x)$  is called the *drift* term. It describes the deterministic part of the evolution of  $x$ .  $g(x)$  is called the *diffusion* term or multiplicative noise. It dictates how the amplitude of noise varies as a function of  $x$ .  $\eta(t)$  is uncorrelated Gaussian noise with zero mean and unit variance. This sort of framework is called *stochastic differential equations* (SDE).

It is possible to approximate the functions in equation 3.2 using time-series data [Jhawar and Guttal (2020)]. Let  $F(x)$  be an approximation of  $f(x)$ . We have:

$$F(x) = \left\langle \frac{X(t + \Delta t) - X(t)}{\Delta t} \right\rangle_{X(t) \in [x, x+\epsilon]}$$

here,  $X(t)$  is the observed value of a quantity  $x$  at time  $t$ . We tolerate some deviation  $\epsilon$  since observed quantities will never be exactly equal to a given value of  $x$ . This quantity is called the *first jump moment*. It is the average change per unit time of the dynamical variable when it is near  $x$ . Similarly, let  $G(x)$  be an approximation of  $g(x)$ . We have:

$$G^2(x) = \left\langle \frac{R^2(x)}{\Delta t} \right\rangle$$

where  $R(x)$  is known as the *residue*:

$$R(x) = (X(t + \Delta t) - X(t))_{X(t) \in [x, x+\epsilon]} - F(x)\Delta t$$

The term inside the brackets is the observed change in time  $\Delta t$  whereas  $F(x)\Delta t$  is the expected change. Hence,  $R(x)$  is the ‘error’.

We aspire to determine  $f(x)$  and  $g(x)$  when  $x$  denotes cluster sizes. We make the assumption that cluster sizes are continuous in nature. Given the observation that cluster sizes in nature (as well as in simulations) span several orders of magnitude, this is a valid assumption to make. Since our data is spatial in nature, we cannot directly use the framework provided above.

We begin by simulating a single step of the models described in chapter 2. If the lattice has been modified, then we calculate the change using the algorithm given in section 3.1. For every cluster size, we maintain a list of changes that it has undergone:

- If a cluster of size  $x$  grows, then a change of  $+1$  is added to the list of cluster size  $x$ . Similarly, if a cluster of size  $x$  decays, then a change of  $-1$  is added to the list of

cluster size  $x$ .

- If clusters of sizes  $\{x_i\}$  have merged to form a cluster of size  $x_f$ , then a change of  $x_f - \max(\{x_i\})$  is added to the list of cluster size  $\max(\{x_i\})$ .
- If a cluster of size  $x_i$  has split into clusters of sizes  $\{x_f\}$ , then a change of  $\max(\{x_f\}) - x_i$  is added to the list of cluster size  $x_i$ .
- If a cluster has appeared, then a change of  $+1$  is added to the list of cluster size  $0$ . Similarly, if a cluster has disappeared, then a change of  $-1$  is added to the list of cluster size  $1$ .

We repeat the above steps for many more iterations of the model, thereby growing the changes list for all cluster sizes. Finally, we calculate the mean of this list as a function of  $x$ . This is an estimate of  $f(x)$ . We calculate the mean of the squared elements of this list as a function of  $x$ . This is an estimate of  $g^2(x)$ .

# Chapter 4

## Results

The next three sections discuss results regarding the cluster size distribution, cluster dynamics and the SDE discovery for cluster sizes. For these sections, we will discuss the results for TDP model only (TDP for  $q = 0$  is identical to contact process). In the last section, we compare the results obtained from TDP model against the control (null models for both cluster size distribution and cluster dynamics)

For all results in the next 3 sections, a landscape of size  $100 \times 100$  was initialized, and the model was equilibrated for  $1000N^2$  iterations ( $N = 100$ ). After equilibration, the model was simulated for further  $1000N^2$  iterations during which the cluster dynamics is tracked according to the algorithm described in 3.1.

The simulation part generates the results required for sections 4.2 and 4.3. The distribution of cluster sizes at the end of the simulation is utilized in section 4.1. Totally, 111 ensembles were simulated, and the results were averaged across them.

**Note about figures:** In every  $2 \times 4$  figure in this chapter, the first column represents the system far from the percolation threshold (but above the critical threshold). The second column represents the system close to the percolation threshold. In the third column, the system is at the percolation threshold, whereas in the fourth column, the system is beyond the percolation threshold.

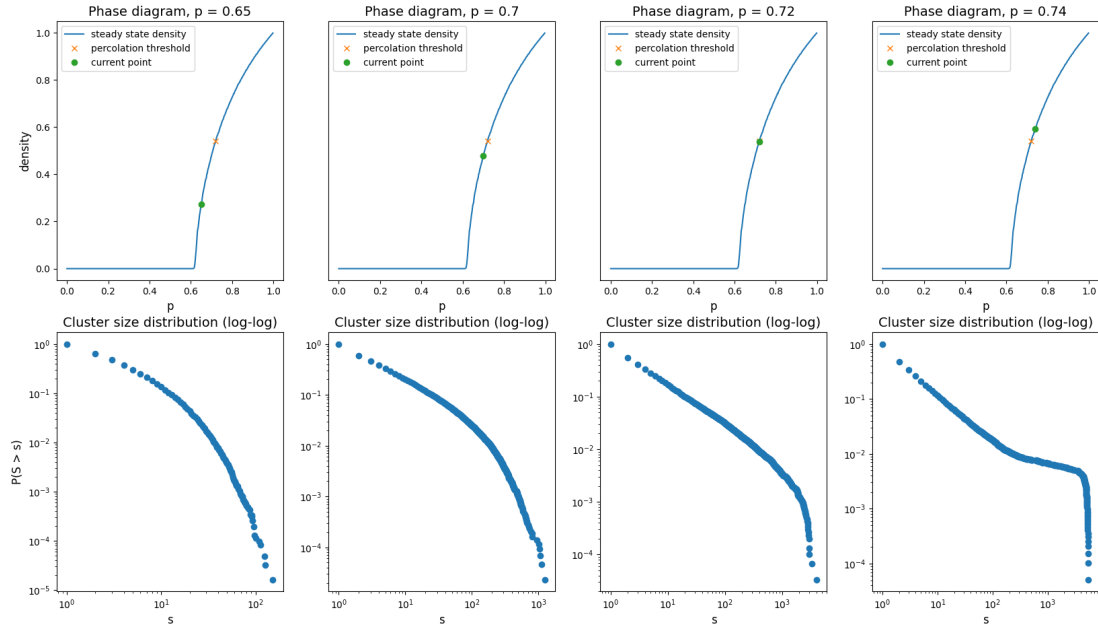


Figure 4.1: Variation of cluster size distribution across the  $q = 0$  percolation threshold of TDP model

## 4.1 Cluster Size Distribution

We analyse how the cluster size distribution changes as the system crosses the percolation threshold. Figure 4.1 showcases the change in cluster size distribution across the percolation threshold of  $q = 0$ . The percolation threshold lies at  $p = 0.72$ .

In figure 4.2, we showcase the change in detail. At the percolation threshold, a few ensembles have began to give rise to percolating clusters. This is conveyed by a few data points being close to  $10^4$  (which corresponds to the area of the system). Also observe the perfect power-law behaviour across three orders of magnitude. Beyond the percolation threshold, all ensembles have sprouted percolating clusters.

The next few figures showcase the variation of cluster size distribution across the percolation thresholds of  $q = 0.25, 0.5, 0.75, 0.92$

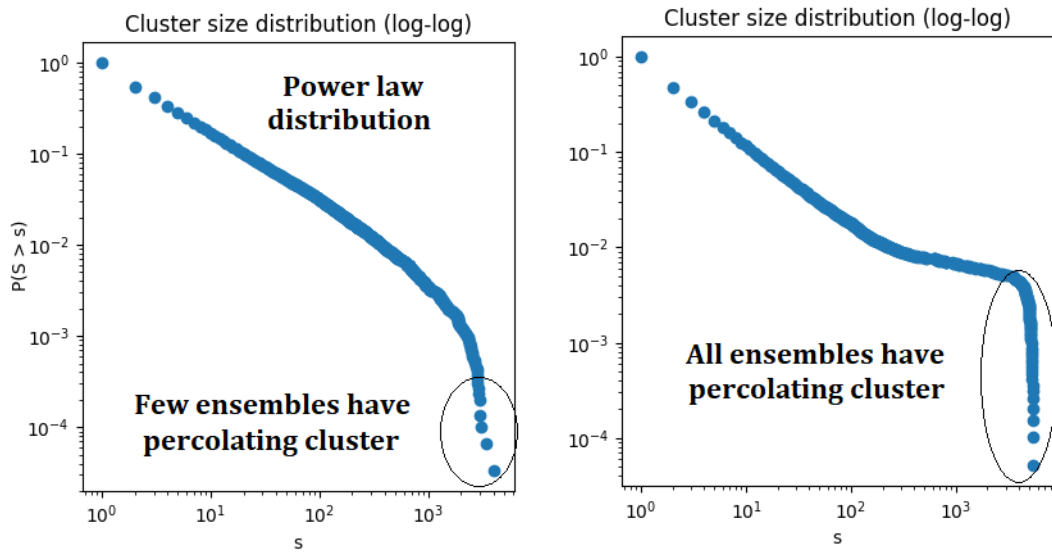


Figure 4.2: Cluster size distribution across the percolation threshold  
(Left) system at percolation threshold. (Right) system beyond percolation threshold

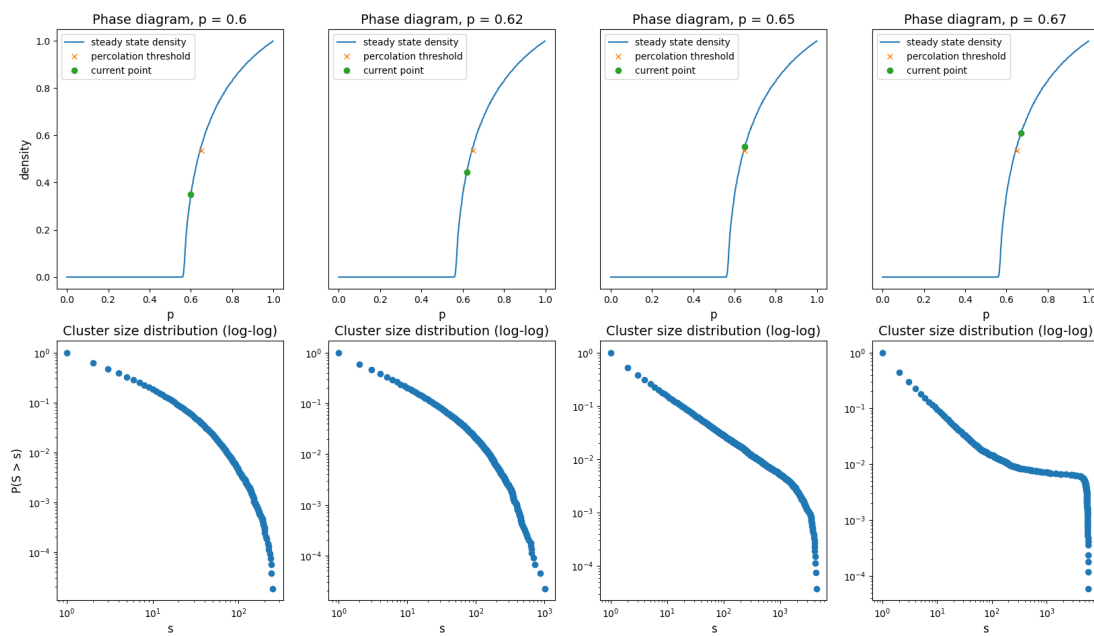


Figure 4.3: Variation of cluster size distribution across the  $q = 0.25$  percolation threshold of TDP model

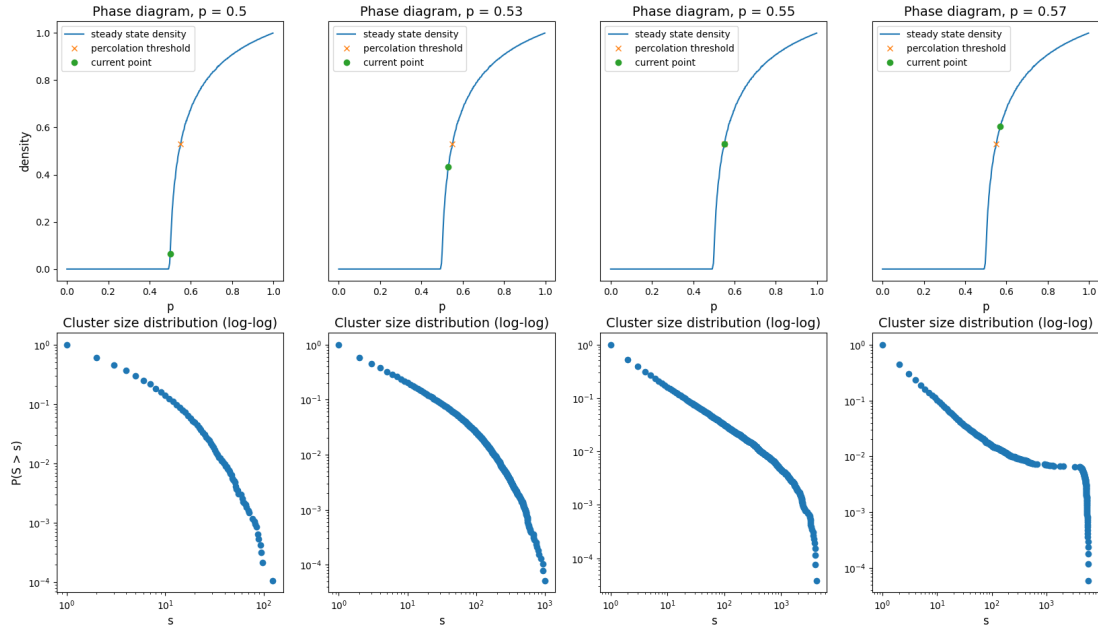


Figure 4.4: Variation of cluster size distribution across the  $q = 0.5$  percolation threshold of TDP model

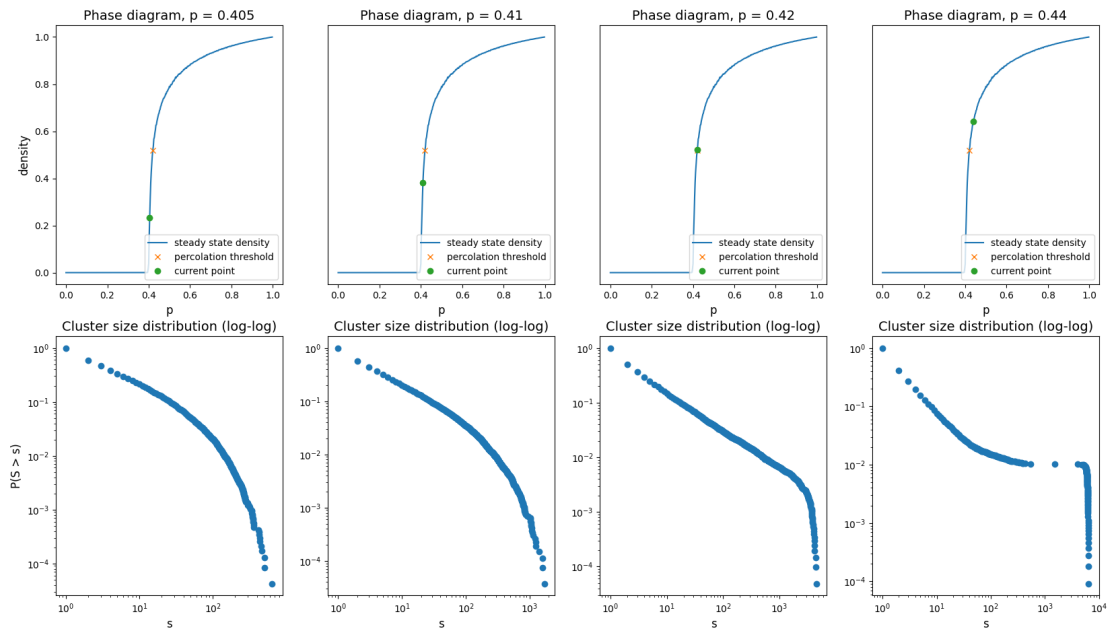


Figure 4.5: Variation of cluster size distribution across the  $q = 0.75$  percolation threshold of TDP model

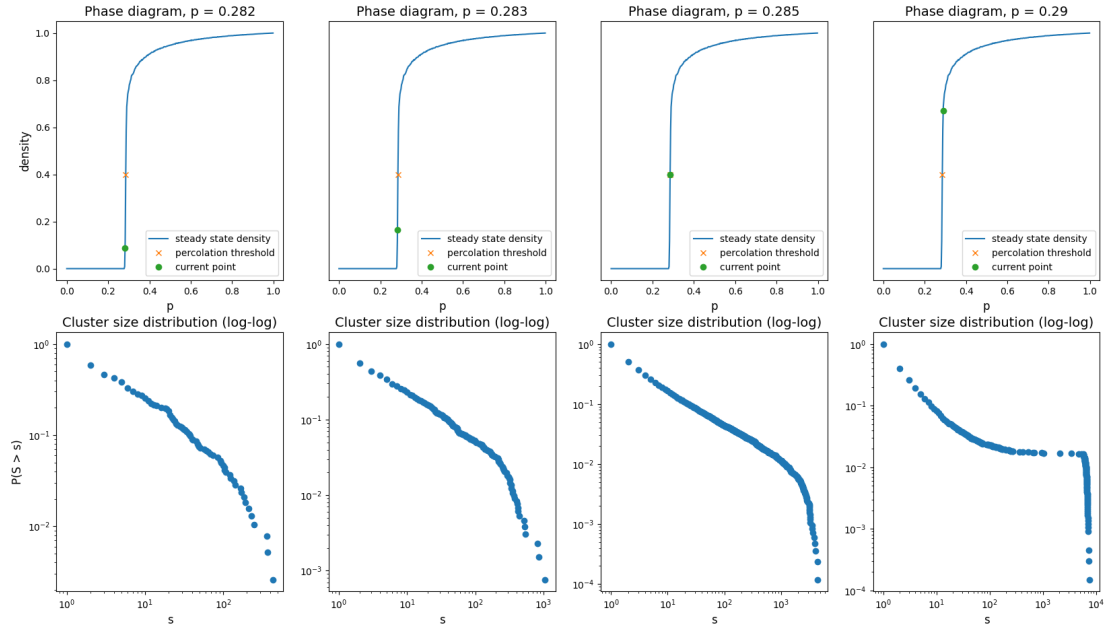


Figure 4.6: Variation of cluster size distribution across the  $q = 0.92$  percolation threshold of TDP model

## 4.2 Cluster Dynamics

Now, we look at the distribution of the changes in cluster sizes (henceforth called ‘cluster dynamics’). The format is same as before. Since this is uncharted territory, we don’t know whether this quantity follows a power-law distribution or an exponential distribution. Hence, we plot log-log graphs, as well as semilog (log on Y-axis only) graphs.

Figure 4.7 showcases the variation in cluster dynamics across the  $q = 0$  percolation threshold. At first glance, we notice that this quantity follows an exponential distribution below the percolation threshold. At (and above) the percolation threshold, we notice a power-law distribution across three orders of magnitude, followed by an exponential decay.

The next few figures showcase the variation of cluster dynamics across the percolation thresholds of  $q = 0.25, 0.5, 0.75, 0.92$

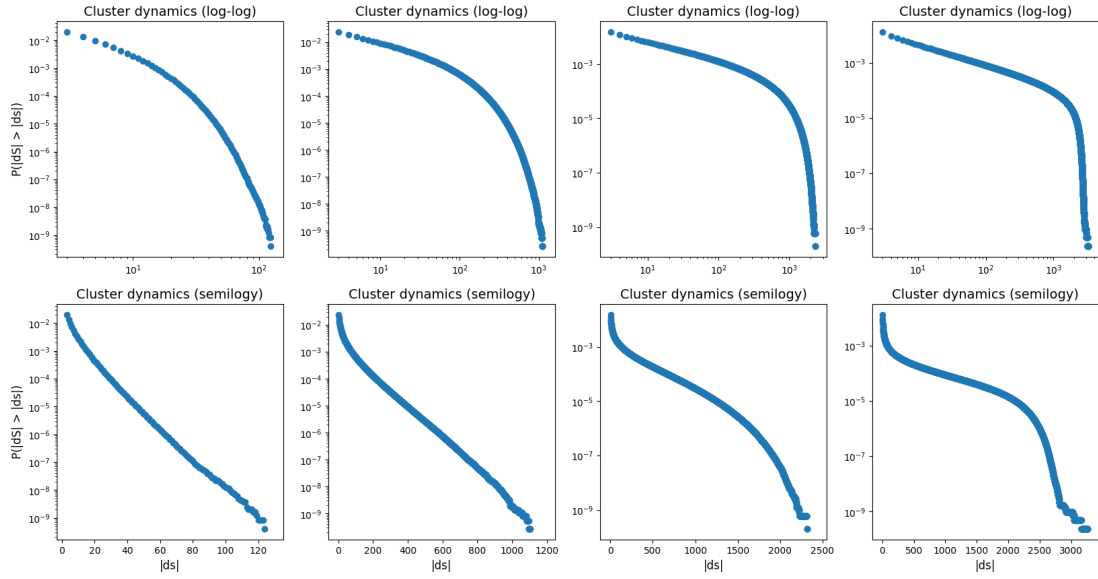


Figure 4.7: Variation of cluster dynamics across the  $q = 0$  percolation threshold of TDP model  
Left to right:  $p = 0.65, 0.7, 0.72, 0.74$

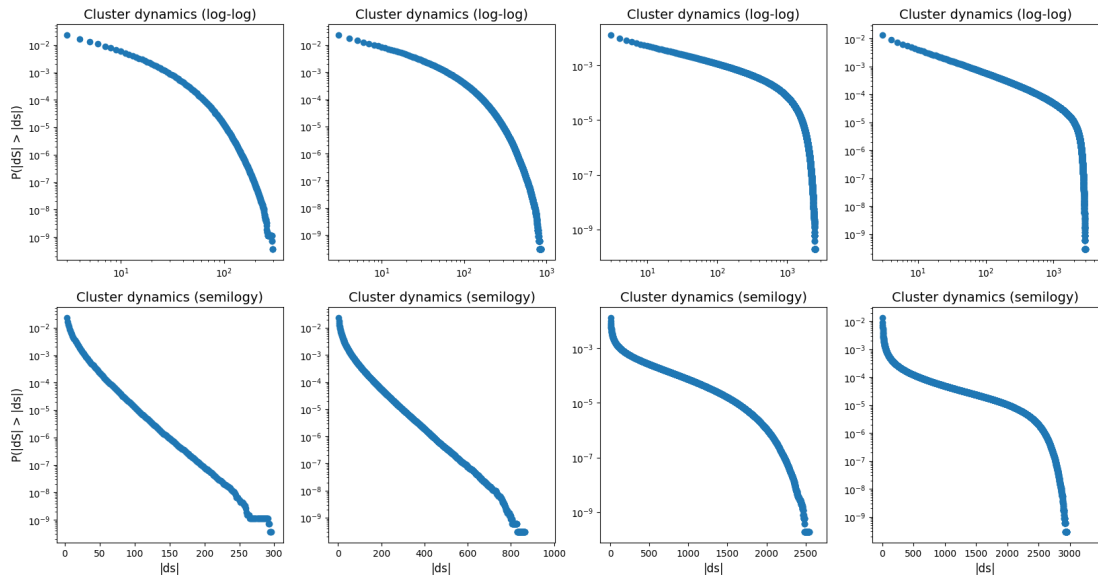


Figure 4.8: Variation of cluster dynamics across the  $q = 0.25$  percolation threshold of TDP model  
Left to right:  $p = 0.6, 0.62, 0.65, 0.67$

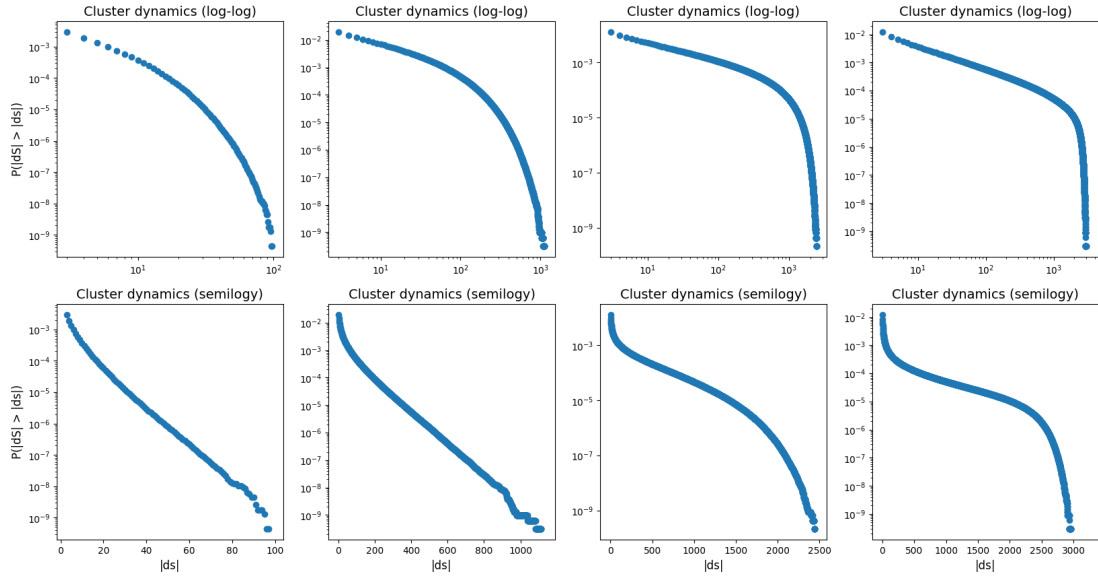


Figure 4.9: Variation of cluster dynamics across the  $q = 0.5$  percolation threshold of TDP model  
Left to right:  $p = 0.5, 0.53, 0.55, 0.57$

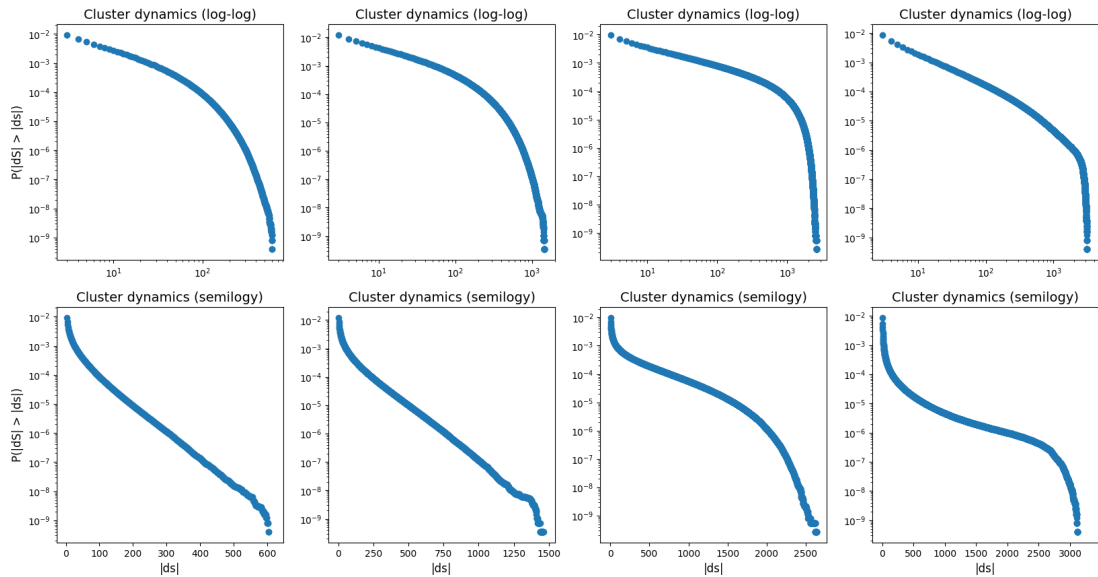


Figure 4.10: Variation of cluster dynamics across the  $q = 0.75$  percolation threshold of TDP model  
Left to right:  $p = 0.405, 0.41, 0.42, 0.44$

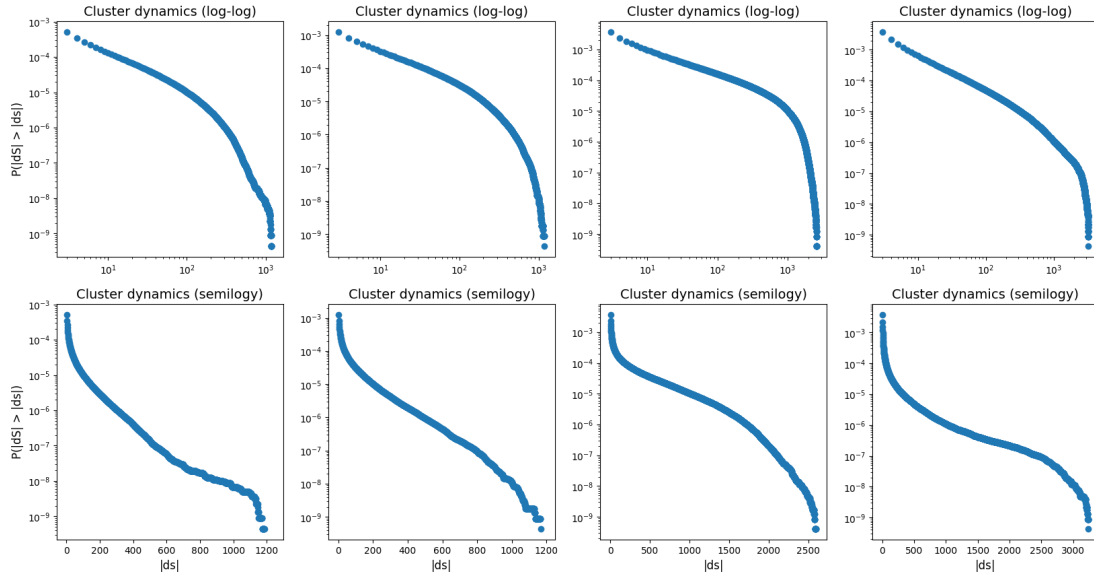


Figure 4.11: Variation of cluster dynamics across the  $q = 0.92$  percolation threshold of TDP model

Left to right:  $p = 0.282, 0.283, 0.285, 0.29$

### 4.3 SDE Discovery for Cluster Sizes

As discussed in section 3.3, mean change in cluster size serves as an approximation for  $f(x)$  (the *drift* term) whereas the mean of squares of change in cluster sizes is an approximation for  $g^2(x)$  (the *diffusion* term). The cluster sizes follow the following SDE:

$$\dot{x} = f(x) + g(x)\eta(t)$$

where  $\eta(t)$  is uncorrelated Gaussian noise of zero mean and unit variance. The column order is same as before. The graphs on top depict an approximation of  $f(x)$  whereas the graphs on bottom depict  $g^2(x)$ .

Figure 4.12 depicts the variation of drift and diffusion terms across the percolation threshold of  $q = 0$ :

- a) Near the critical threshold, we see that  $f(x)$  is briefly positive, after which it becomes negative. The system features a low level of noise that increases with cluster size.
- b) Below the percolation threshold, we see that the behaviour of  $f(x)$  is very similar to logistic dynamics ( $f(x) \approx ax - bx^2$ ). The system features a moderate level of noise that still increases with cluster size.
- c) At the percolation threshold, the behaviour of  $f(x)$  becomes complex. However, one interesting observation is that the noise saturates approximately above the point where  $f(x)$  crosses 0.

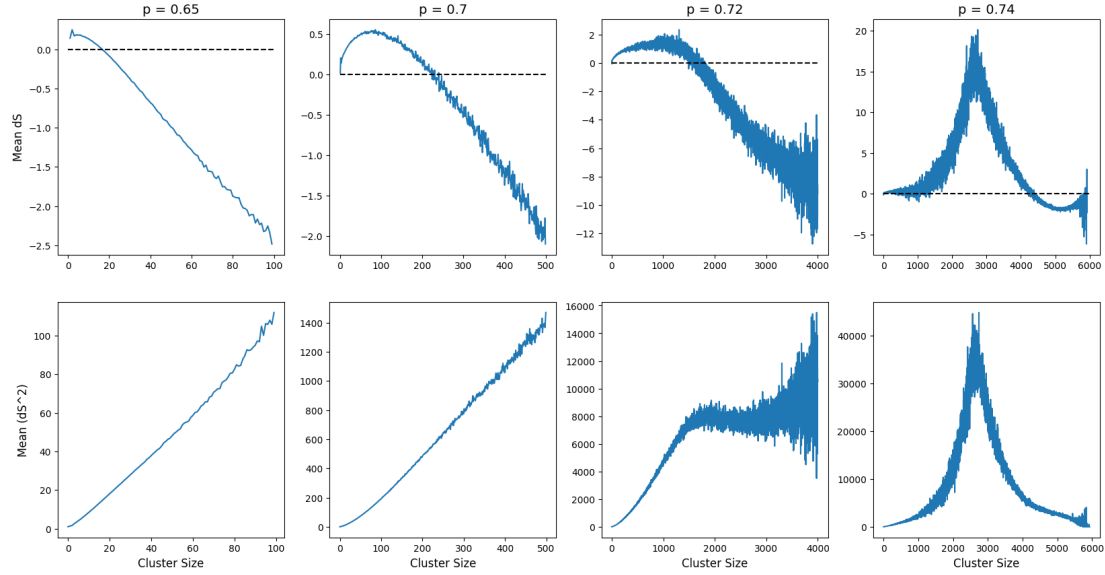


Figure 4.12: Variation of drift and diffusion across the  $q = 0$  percolation threshold of TDP model

- d) Above the percolation threshold, we start to see effects due to the finite size of the landscape. As a small cluster grows, it is more likely to merge with surrounding clusters. Hence, value of  $f(x)$  increases. Beyond the peak, the cluster has probably ran out of surrounding clusters to merge with (due to the finite landscape). The cluster is more likely to split. Hence, value of  $f(x)$  decreases after a maximum.

The next few figures showcase the variation of drift and diffusion terms across the percolation thresholds of  $q = 0.25, 0.5, 0.75, 0.92$

As the positive feedback  $q$  increases, we notice that, below the percolation threshold,  $f(x)$  is initially negative (figures 4.14 and 4.15). This is due to the fact that  $p$  is inherently low to sustain vegetation. However, when the cluster size crosses a certain value, positive feedback amongst the occupied cells of the cluster makes the value of  $f(x)$  positive.

Another remarkable observation is the increase in noise of the system with increasing positive feedback. As explained in section 2.2.2,  $p$  enables two transitions whereas  $q$  is required for two more transitions. Since more transitions are possible with an increase in the value of  $q$ , the system becomes more noisy.

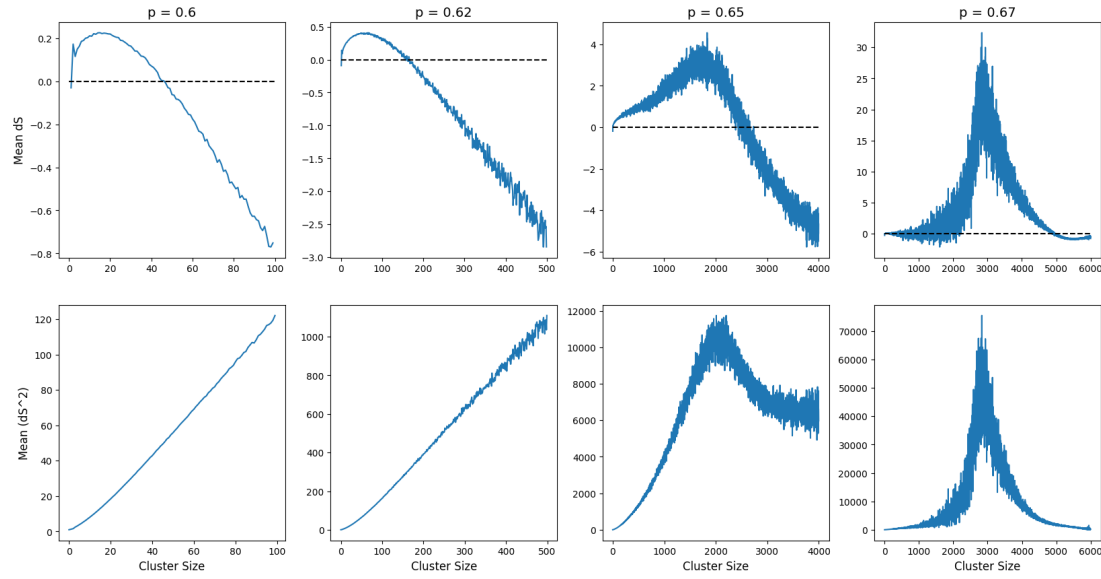


Figure 4.13: Variation of drift and diffusion across the  $q = 0.25$  percolation threshold of TDP model

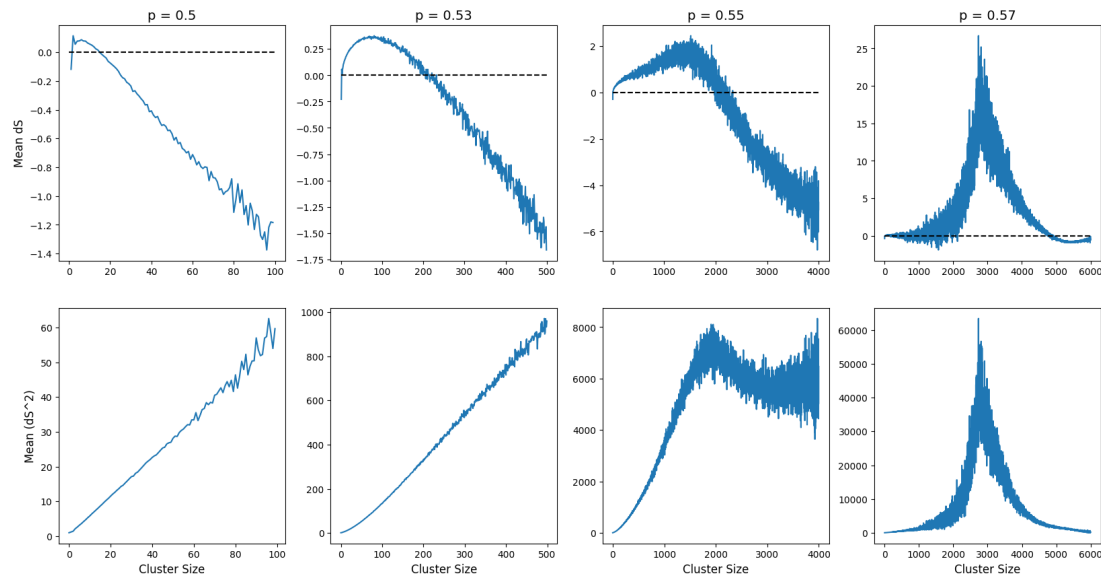


Figure 4.14: Variation of drift and diffusion across the  $q = 0.5$  percolation threshold of TDP model

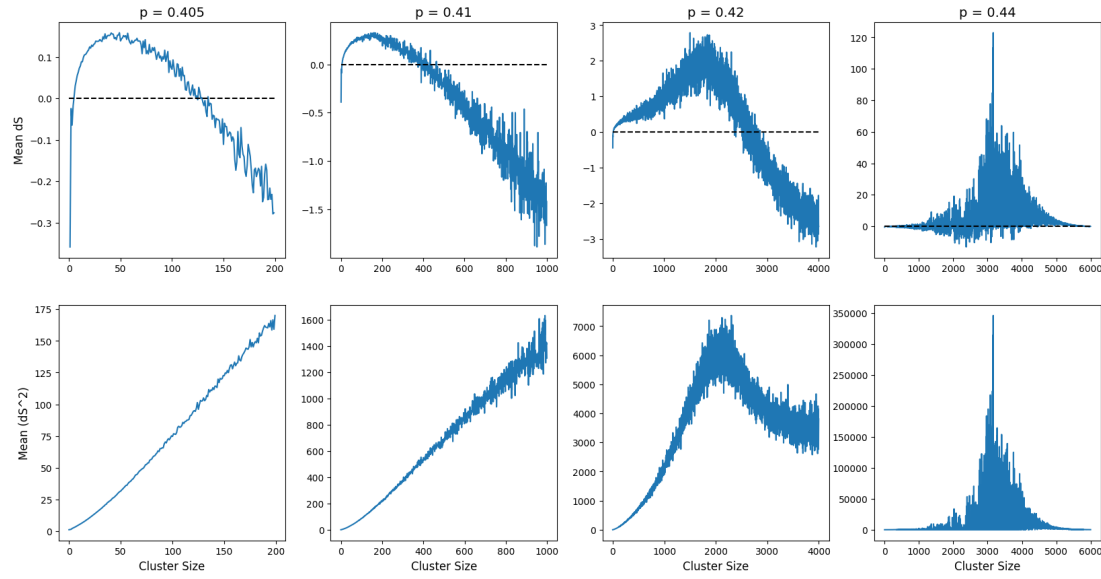


Figure 4.15: Variation of drift and diffusion across the  $q = 0.75$  percolation threshold of TDP model

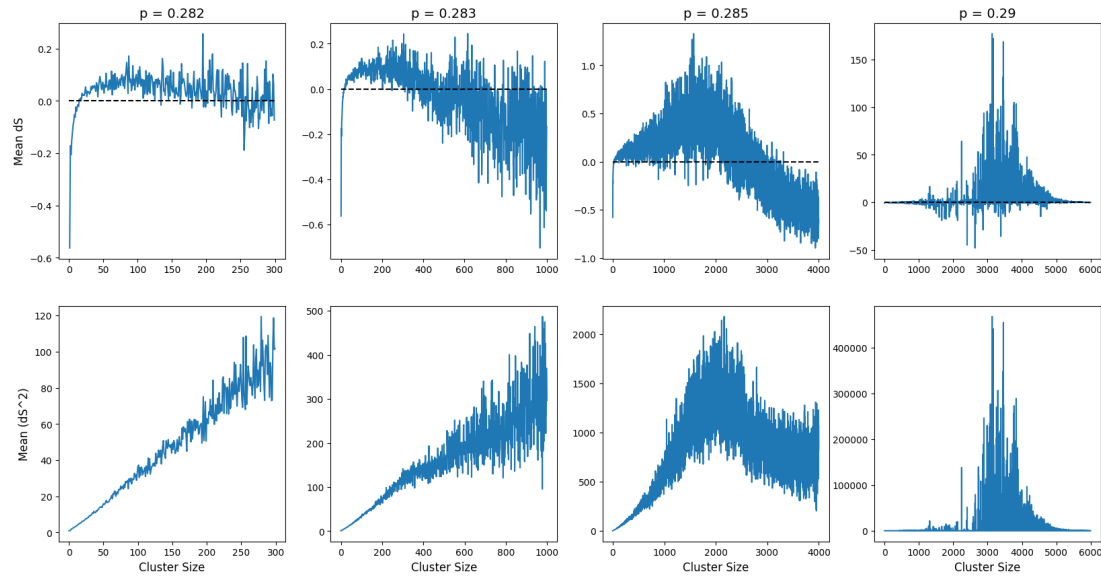


Figure 4.16: Variation of drift and diffusion across the  $q = 0.92$  percolation threshold of TDP model

## 4.4 Comparison with Results from Null Models

We need to compare all our results generated using TDP model against a model that follows no particular dynamics. We utilize the dynamic null model described in section 2.5 since it not only evolves randomly but also gives rise to a random distribution of cluster sizes.

A TDP model simulated using parameters  $(p, q)$  is associated with some steady state density  $\rho$ . We initialize the dynamic null model with this density. By construction, the null model's density tends to stick around the initialized density. We compare the cluster size distribution, cluster dynamics, the drift term and the diffusion term resulting from both the models. We attempt to discern any trends (in the null model) that take place over percolation thresholds of the TDP model. The figures and their corresponding model parameters have been enumerated in table 4.1. Here are some observations:

- a) **Cluster size distribution:** Below (and at) the percolation threshold, the cluster size distribution decays much faster in the null model. Above the percolation threshold, both models have identical cluster size distributions.
- b) **Cluster dynamics:** Same as (a)
- c) **Drift term:** Below (and at) the percolation threshold, the drift term decreases linearly, and decays much faster in the null model. Above the percolation threshold, the drift term behaves similarly in both models. This explains the observation in (a)
- d) **Diffusion term:** Below (and at) the percolation threshold, the diffusion term increases linearly in both models. The rate of increase is appreciably similar. Above percolation threshold, the diffusion term behaves similarly in both models. However, as  $q$  increases, the TDP model features more noise than the null model.

**Note:** At the lower densities, the null model does not feature many clusters of bigger size. Owing to this, tracking the cluster dynamics of bigger clusters is more error prone. This is why their drift and diffusion terms have been cut-off at lower cluster sizes.

Figure	Percolation Threshold	Values of p	Corresponding densities
4.17	$q = 0$	0.65, 0.7, 0.72, 0.74	0.27, 0.48, 0.54, 0.61
4.18	$q = 0.25$	0.6, 0.62, 0.65, 0.67	0.35, 0.45, 0.55, 0.61
4.19	$q = 0.5$	0.5, 0.53, 0.55, 0.57	0.06, 0.43, 0.53, 0.6
4.20	$q = 0.75$	0.405, 0.41, 0.42, 0.44	0.23, 0.38, 0.52, 0.64

Table 4.1: Percolation Thresholds, values of  $p$  and their corresponding densities

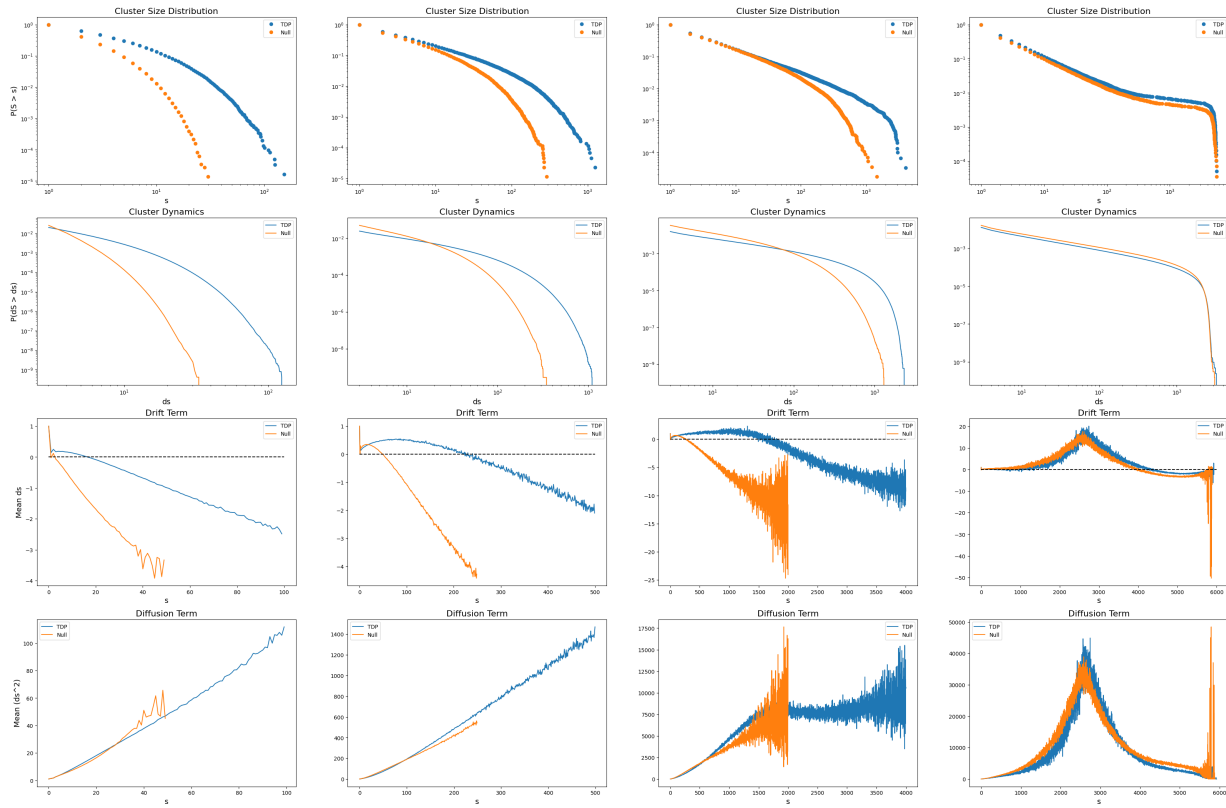


Figure 4.17: Comparison between results of TDP and null model across the  $q = 0$  percolation threshold

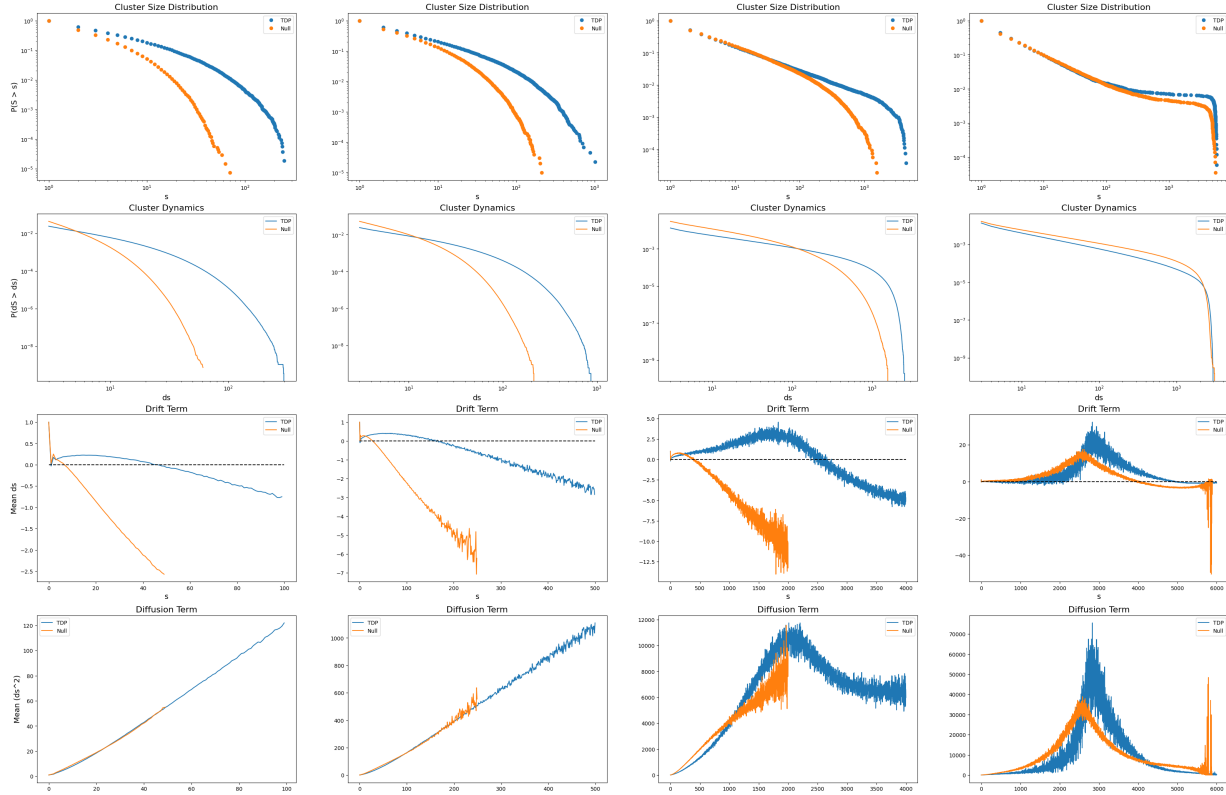


Figure 4.18: Comparison between results of TDP and null model across the  $q = 0.25$  percolation threshold

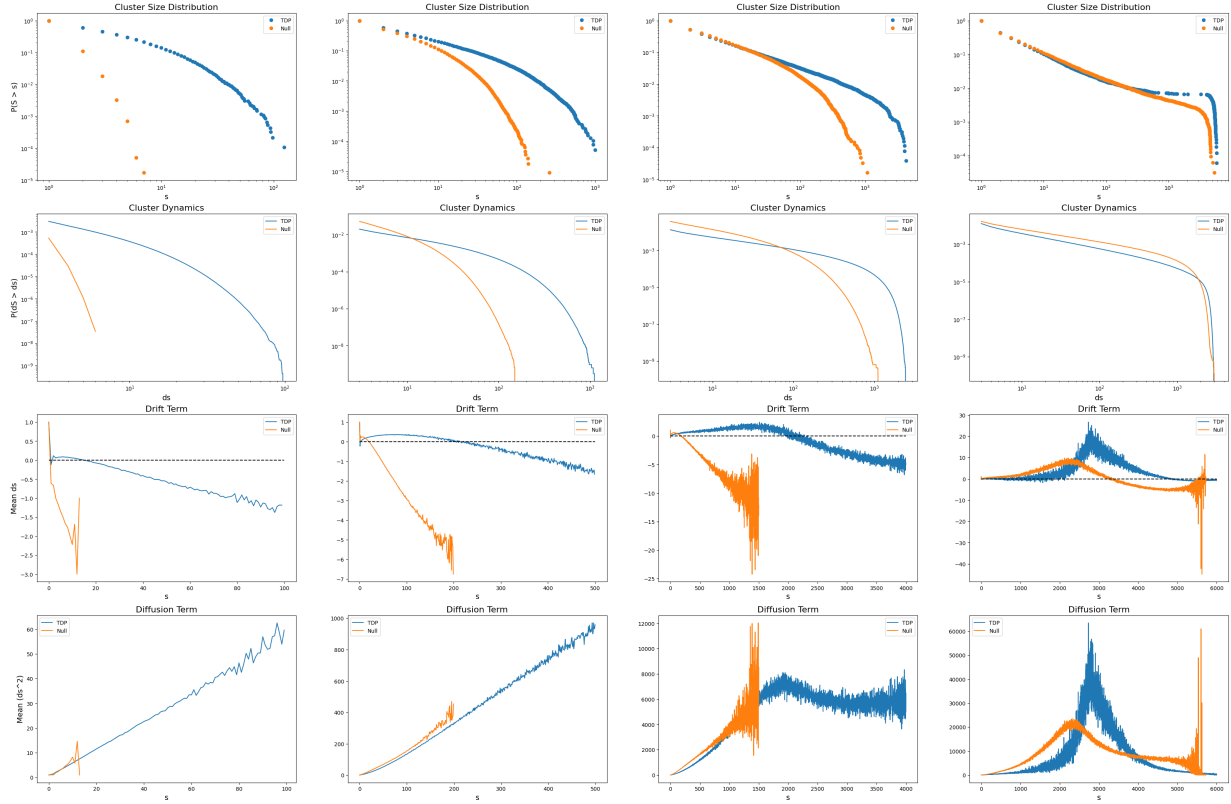


Figure 4.19: Comparison between results of TDP and null model across the  $q = 0.5$  percolation threshold

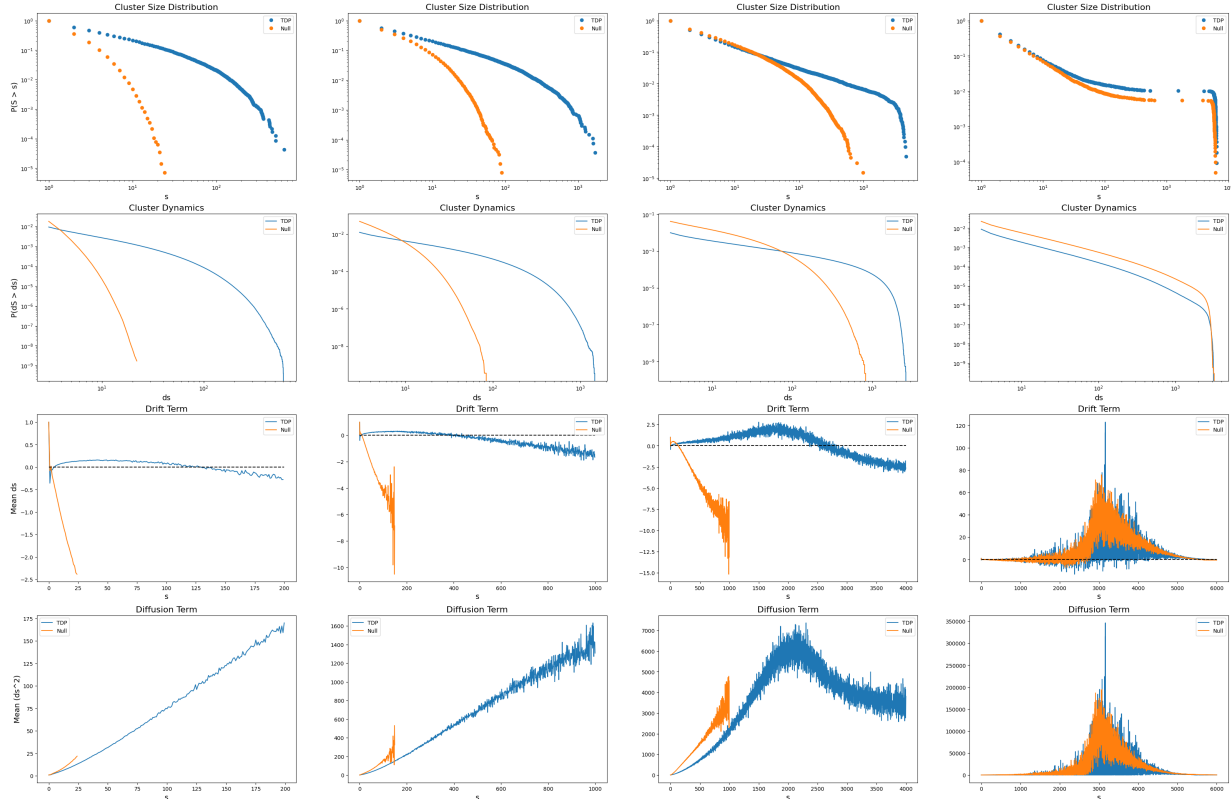


Figure 4.20: Comparison between results of TDP and null model across the  $q = 0.75$  percolation threshold

# Chapter 5

## Discussion

In the results chapter, we have studied how three quantities vary from the critical threshold to the percolation threshold (and beyond), in the TDP model. These quantities are:

- a) Cluster size distribution (section 4.1)
- b) Cluster dynamics (section 4.2)
- c) The drift and diffusion terms (section 4.3)

In section 4.4, we noticed that, beyond the percolation threshold, the TDP model behaves similar to a null model. This suggests that its dynamics is random. Hence, while formulating early warning signals, we should not utilize observations from beyond the percolation threshold.

Based on the trends observed between the critical threshold and percolation threshold, we can formulate three early warning signals. They have been described in the next three sections.

**Note about figures:** In all the  $2 \times 4$  figures of this section, the graphs towards the left depict the system when it is far from the critical threshold. The graphs towards the right depict the system near the critical threshold.

## 5.1 Deviation of cluster size distribution from power-law behaviour near critical thresholds

In figure 4.2, we noted that, at the percolation threshold, a power-law distribution exists across three orders of magnitude. As we go below the percolation threshold, this straight line deteriorates to a curved line that decays faster. This trend has been shown in figure 5.1.

In order to be more rigorous in our approach, we utilize the methods discussed in section 3.2. We fit the cluster size distribution to a power-law, a truncated power-law (TPL) and an exponential distribution. We calculate the BIC values from the log-likelihood of the MLE fit. A distribution with a smaller value of BIC is said to better fit the given data.

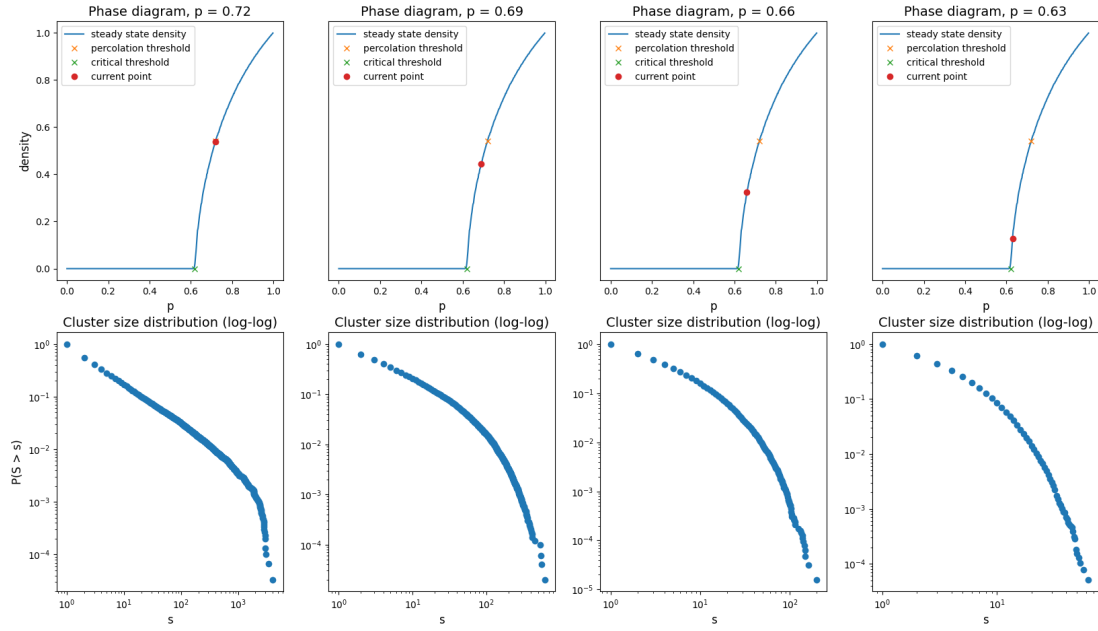
After looking at table 5.1, we propose our first early warning signal:

As a system nears its critical threshold, the cluster size distribution changes from a power-law distribution to a truncated power-law distribution

This result has been empirically observed in [Kéfi et al. (2007a)]. A section of the mediterranean semi-arid vegetation was divided into regions. The grazing pressure received by each region was calculated via GPS tracking of sheep. It was observed that regions with more grazing pressure had a truncated power-law distribution of cluster sizes (since they were closer to a critical threshold).

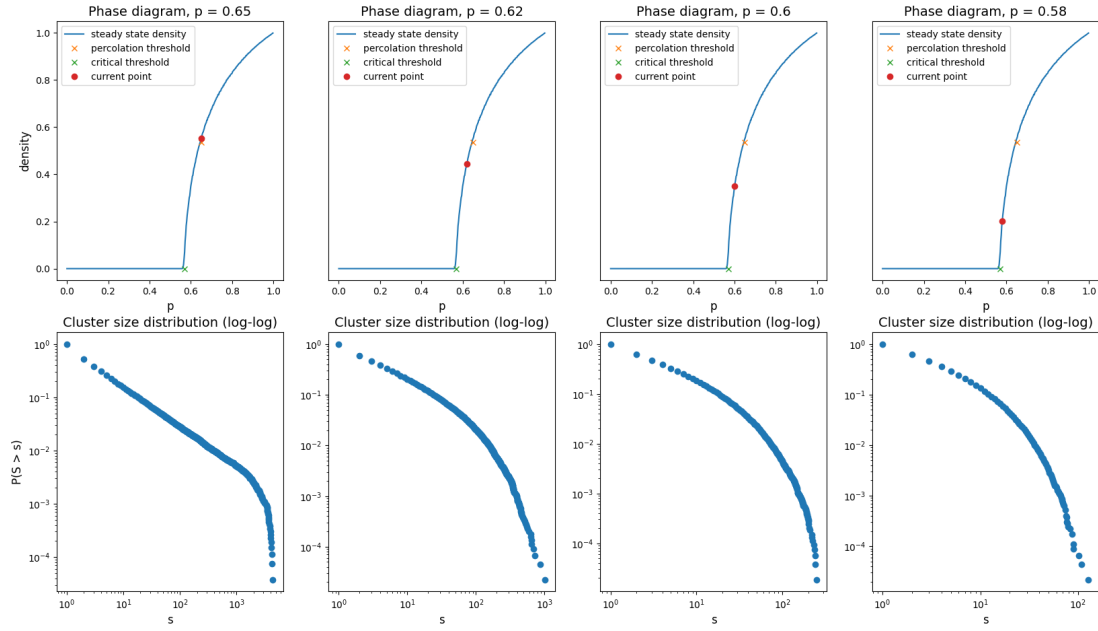
In the TDP model, as the value of  $q$  increases, the percolation threshold comes closer to the critical threshold. For example, at  $q = 0.92$  (high positive feedback), the critical threshold is at  $p \approx 0.28$  whereas the percolation threshold is at  $p \approx 0.285$ . There is a very small range where this early warning signal can be applied. Hence, high positive feedback reduces the utility of this early warning signal. This limitation has been explored in [Sankaran et al. (2019)].

The same trend has been showcased for  $q = 0.25$  and  $q = 0.5$

Figure 5.1: Decay of power-law clustering across near the critical threshold of  $q = 0$ 

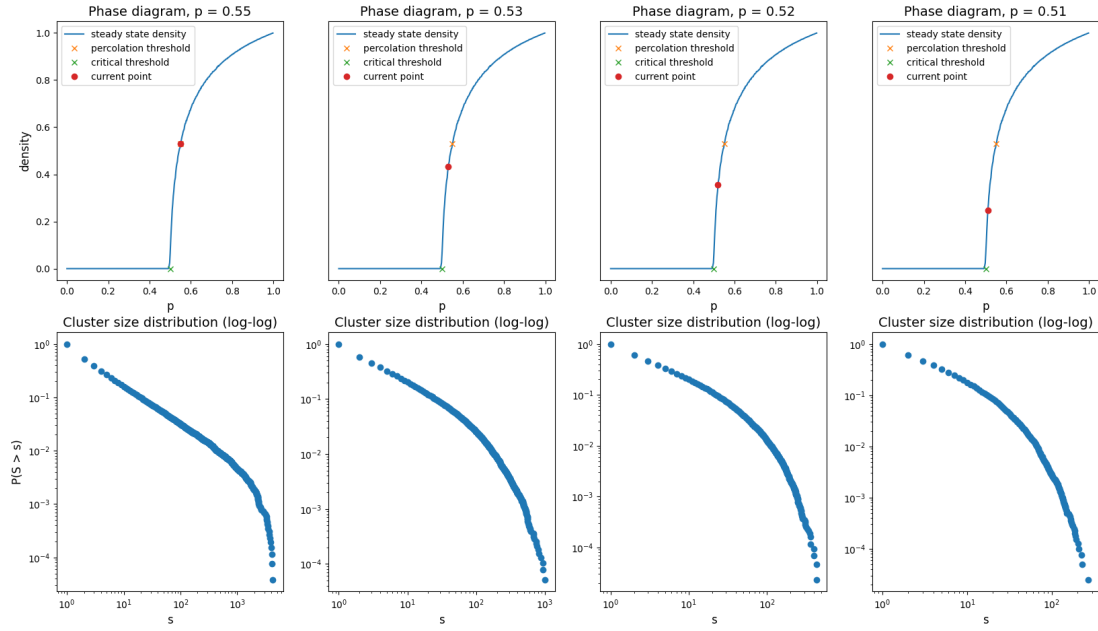
Value of p	BIC of power-law	BIC of TPL	BIC of exp	Best fit
0.62	259	253	287	TPL
0.63	638	636	822	TPL
0.64	858	858	1117	TPL $\approx$ power-law
0.65	1064	1064	1409	TPL $\approx$ power-law
0.66	1316	1315	1759	TPL
0.67	1609	1609	2235	TPL $\approx$ power-law
0.68	2030	2031	2933	power-law
0.69	2439	2442	3684	power-law
0.70	2867	2872	4648	power-law
0.71	3027	3034	5609	power-law
0.72	2731	2739	5801	power-law

Table 5.1: BIC values obtained from fitting cluster size distributions across the  $q = 0$  percolation threshold

Figure 5.2: Decay of power-law clustering across near the critical threshold of  $q = 0.25$ 

Value of p	BIC of power-law	BIC of TPL	BIC of exp	Best fit
0.57	604	604	727	TPL $\approx$ power-law
0.58	974	973	1243	TPL
0.59	1355	1355	1866	TPL $\approx$ power-law
0.6	1761	1761	2564	TPL $\approx$ power-law
0.61	2170	2172	3302	power-law
0.62	2624	2628	4182	power-law
0.63	2981	2987	5329	power-law
0.64	2956	2406	5847	power-law
0.65	2398	2406	5371	power-law

Table 5.2: BIC values obtained from fitting cluster size distributions across the  $q = 0.25$  percolation threshold

Figure 5.3: Decay of power-law clustering across near the critical threshold of  $q = 0.5$ 

Value of p	BIC of power-law	BIC of TPL	BIC of exp	Best fit
0.5	670	667	859	TPL
0.51	1478	1478	2059	$\text{TPL} \approx \text{power-law}$
0.52	2158	2158	3177	$\text{TPL} \approx \text{power-law}$
0.53	2708	2713	4450	power-law
0.54	2948	2954	5578	power-law
0.55	2543	2550	5491	power-law
0.56	1828	1837	4274	power-law
0.57	1306	1314	3194	power-law

Table 5.3: BIC values obtained from fitting cluster size distributions across the  $q = 0.5$  percolation threshold

## 5.2 Exponential behaviour of cluster dynamics near critical thresholds

In section 4.2, we looked at variation of cluster dynamics across percolation thresholds. Since we don't know (beforehand) the best distribution that fits this data, we plotted cluster dynamics on a log-log scale as well as a semi-log scale (log on Y-axis only). One might notice that the semi-log graphs are appreciably straight for lower values of  $p$  (for example, see the bottom left plot in figure 4.7). This suggests a prospective early warning signal.

On comparing goodness of fit between power-law, truncated power-law and exponential distributions (using the methods described in section 3.2), we find that the exponential distribution better fits the data for all values of  $p$  between the critical and percolation thresholds. For evaluating goodness of an exponential fit alone, we merely calculate the  $R^2$  score from the linear fit of a semi-log plot.

We showcase this trend in figure 5.4. For demonstration purposes, the trend has been shown for a few values of  $p$ . However, the variation of  $R^2$  has been plotted as a function of many values of  $p$ , in figure 5.5. Now, we propose our second warning signal:

A system with an exponential behaviour in its cluster dynamics has crossed the percolation threshold and is poised to undergo a critical transition

While this early warning signal is not particularly useful for lower values of positive feedback (when the critical and percolation thresholds are far from each other), it finds a utility in higher values of positive feedback (when percolation threshold is very close to the critical threshold). In a way, it fills the void left by the signal discussed in the previous section.

To the best of the author's knowledge, no paper in literature has looked at fine-grained cluster dynamics of patchy ecosystems, let alone propose an early warning signal based on it. The same trend has been showcased for  $q = 0.25$  and  $q = 0.5$

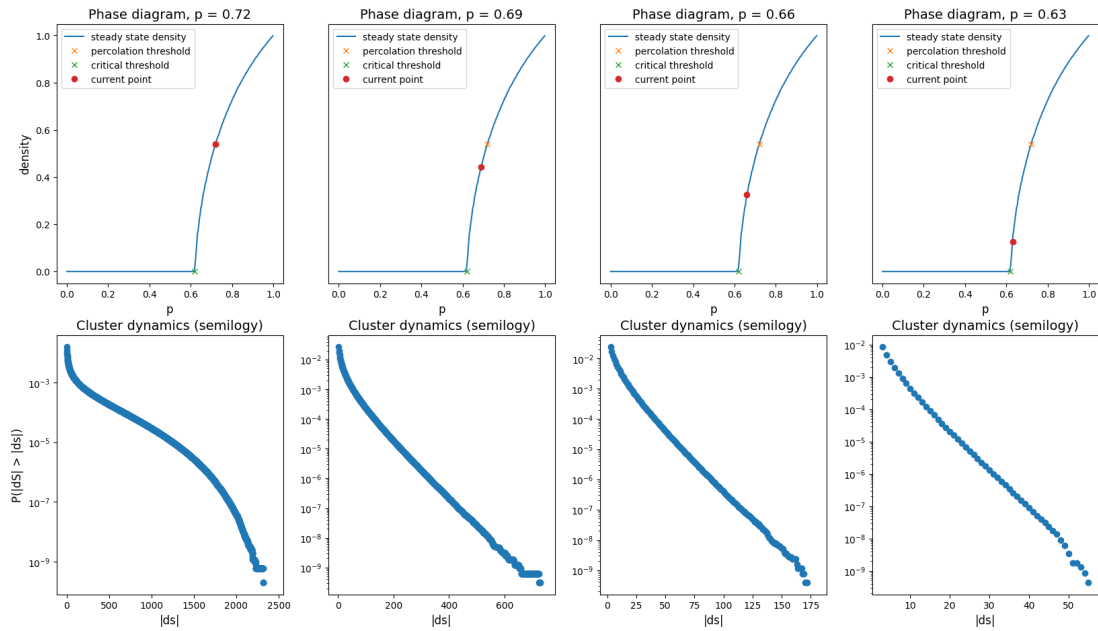


Figure 5.4: Exponential behaviour of cluster dynamics near critical threshold of  $q = 0$

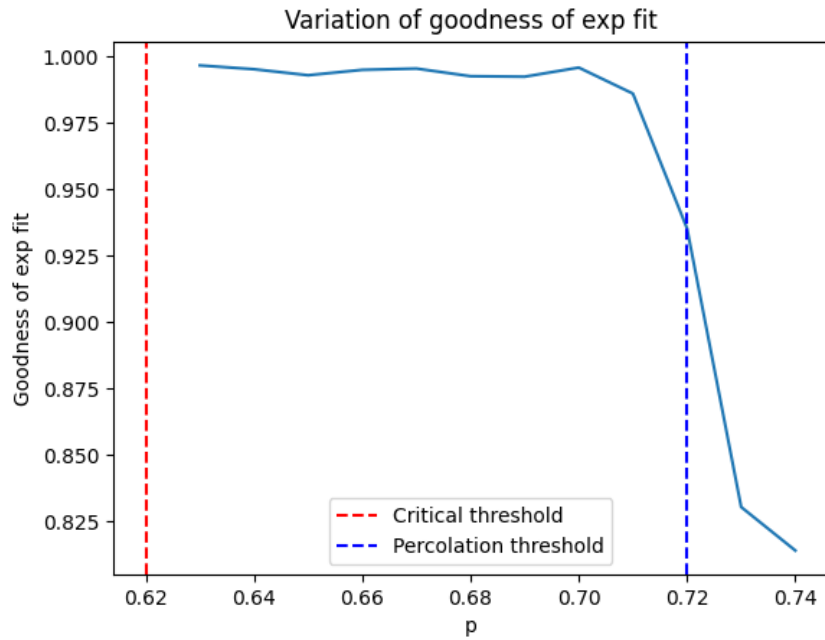


Figure 5.5: Increase in goodness of exp fit below percolation threshold of  $q = 0$

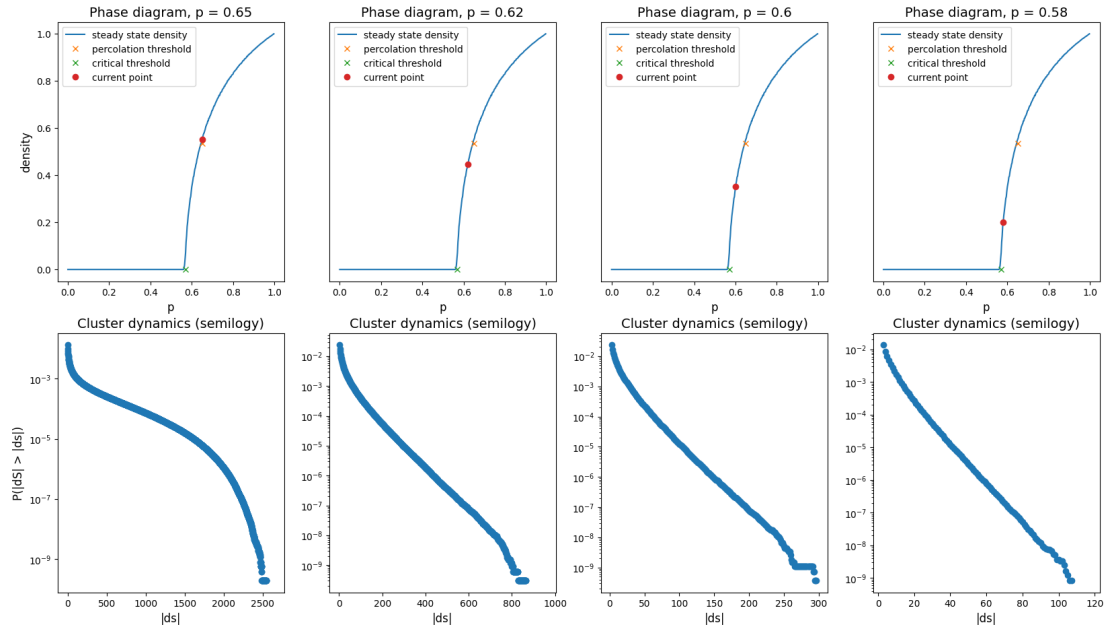


Figure 5.6: Exponential behaviour of cluster dynamics near critical threshold of  $q = 0.25$

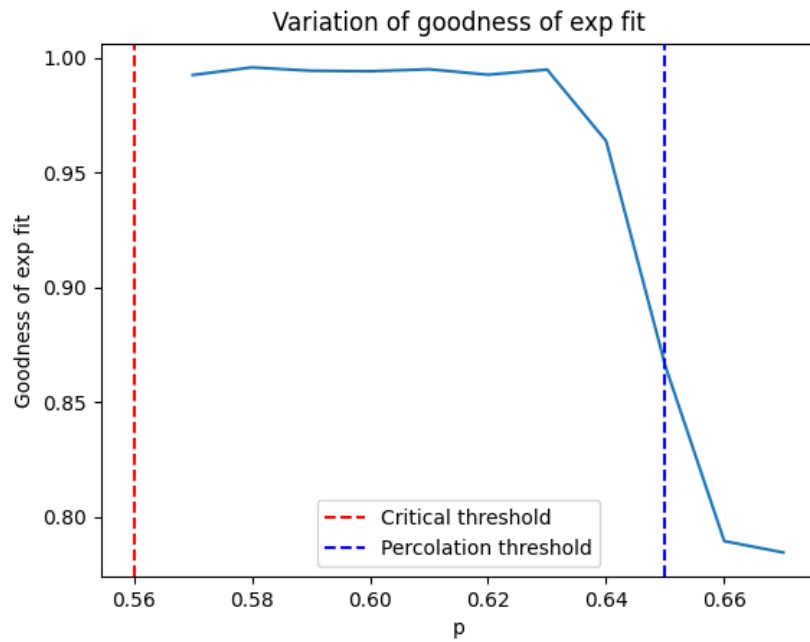


Figure 5.7: Increase in goodness of exp fit below percolation threshold of  $q = 0.25$

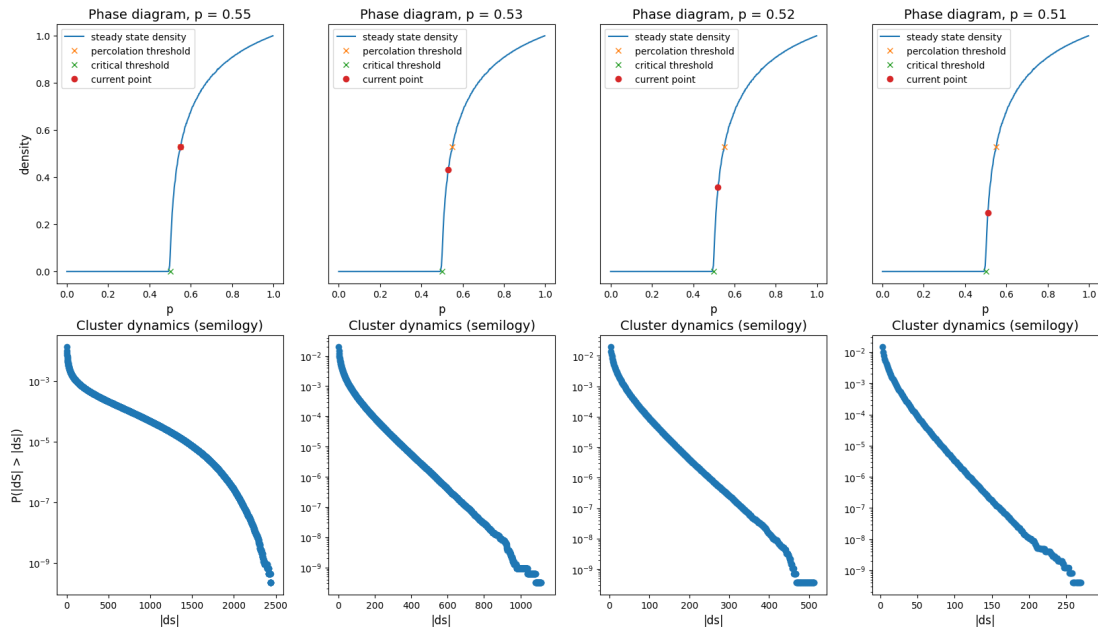


Figure 5.8: Exponential behaviour of cluster dynamics near critical threshold of  $q = 0.5$

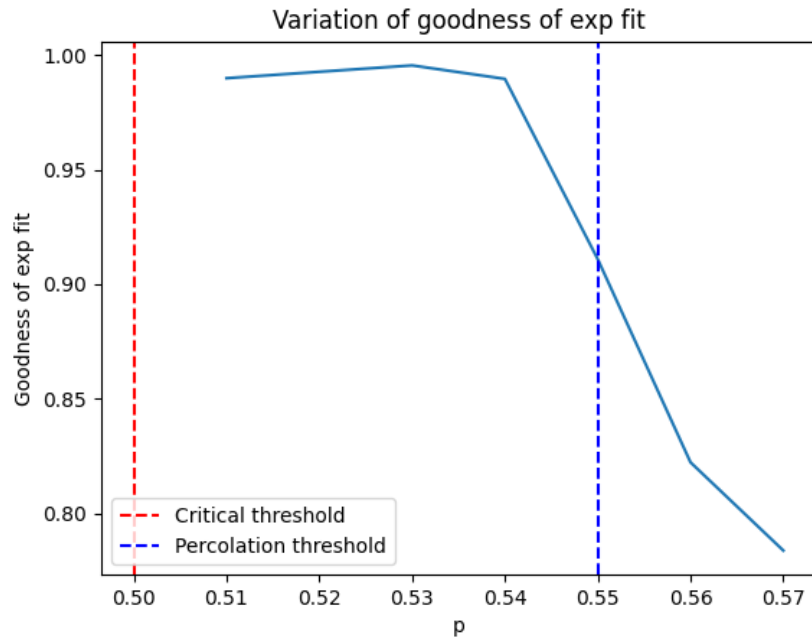


Figure 5.9: Increase in goodness of exp fit below percolation threshold of  $q = 0.5$

### 5.3 Rapid decrease in critical cluster size near critical thresholds

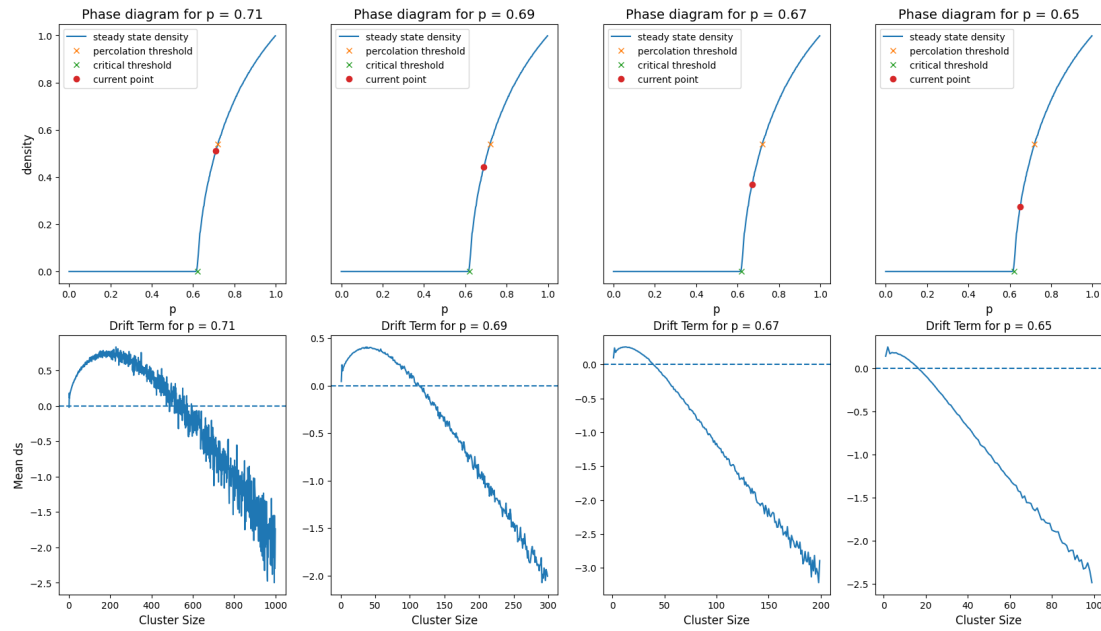
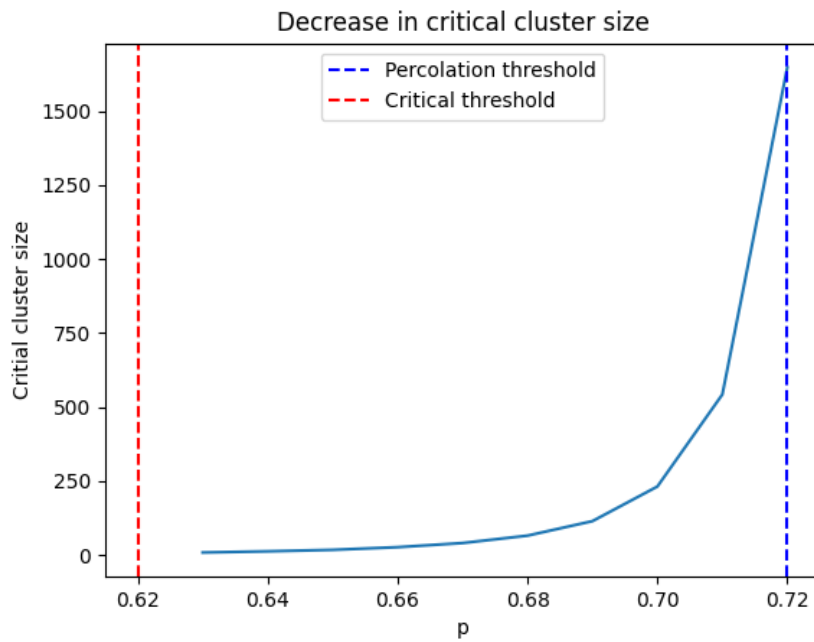
In section 4.3, we noted that, below the percolation threshold,  $f(x)$  (the drift term) is initially positive but becomes negative later (for example, refer the top left graph in figure 4.12). Hence, there is some cluster size which is expected to neither grow nor decay (in the absence of noise). This is called the *critical cluster size*.

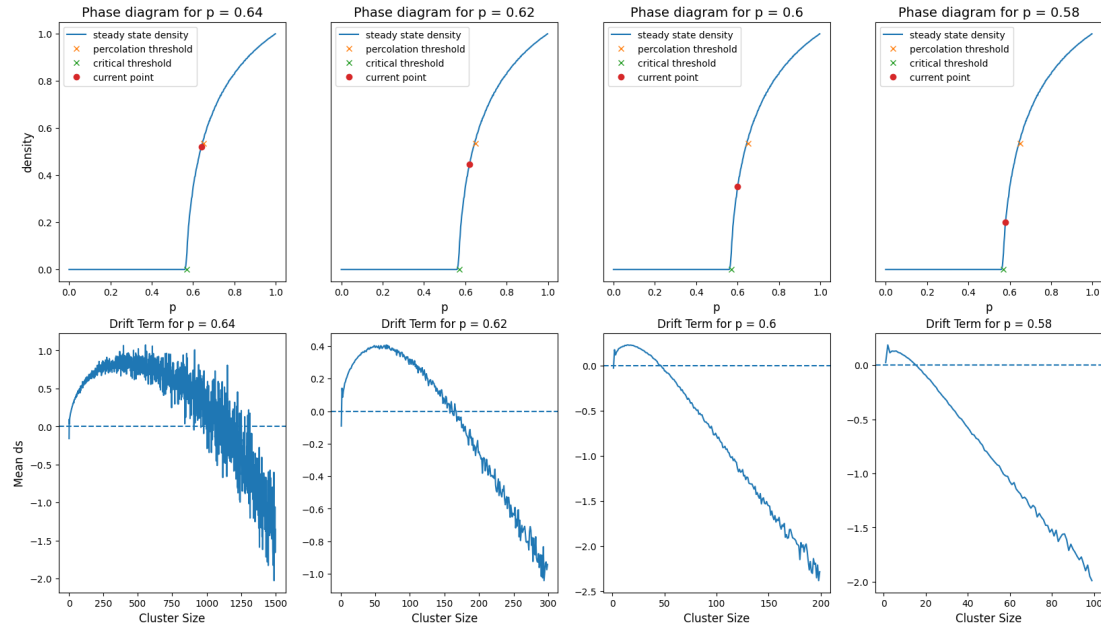
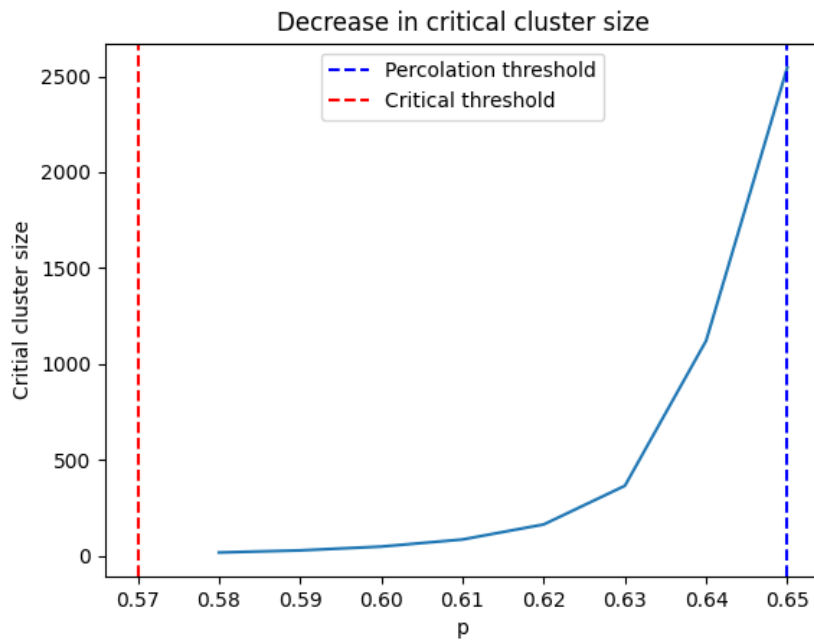
For lower values of positive feedback, only one fixed point was observed. This fixed point is stable, because any cluster that is bigger than this fixed point decays, whereas any cluster that is smaller than this fixed point grows. At higher values of positive feedback, we noticed another fixed point (refer top left graph in figure 4.15). This fixed point is unstable. For our purpose, we shall focus on the former (stable) fixed point only. We observe that the critical cluster size decreases as the system comes closer to its critical threshold.

We showcase this trend in figure 5.10. For demonstration purposes, this trend has been shown for a few values of  $p$ . However, the variation of critical cluster size has been plotted as a function of many values of  $p$ , in figure 5.11. Now, we propose our third (and final) warning signal:

As a system nears its critical threshold, the stable fixed point of its drift function (i.e. the critical cluster size) rapidly decreases

Critical cluster size has been explored in [Weissmann and Shnerb (2016)]. However, they only looked at the probability of growth/decay of a particular cluster size. The point at which these two probabilities converge was deemed to be the critical cluster size. On the other hand, we have calculated the critical cluster size in a much more accurate manner, by intricately peering into the dynamics of the system. The same trend has been showcased for  $q = 0.25$  and  $q = 0.5$

Figure 5.10: Variation in fixed point near the critical threshold of  $q = 0$ Figure 5.11: Decrease in critical cluster size near the critical threshold of  $q = 0$

Figure 5.12: Variation in fixed point near the critical threshold of  $q = 0.25$ Figure 5.13: Decrease in critical cluster size near the critical threshold of  $q = 0.25$

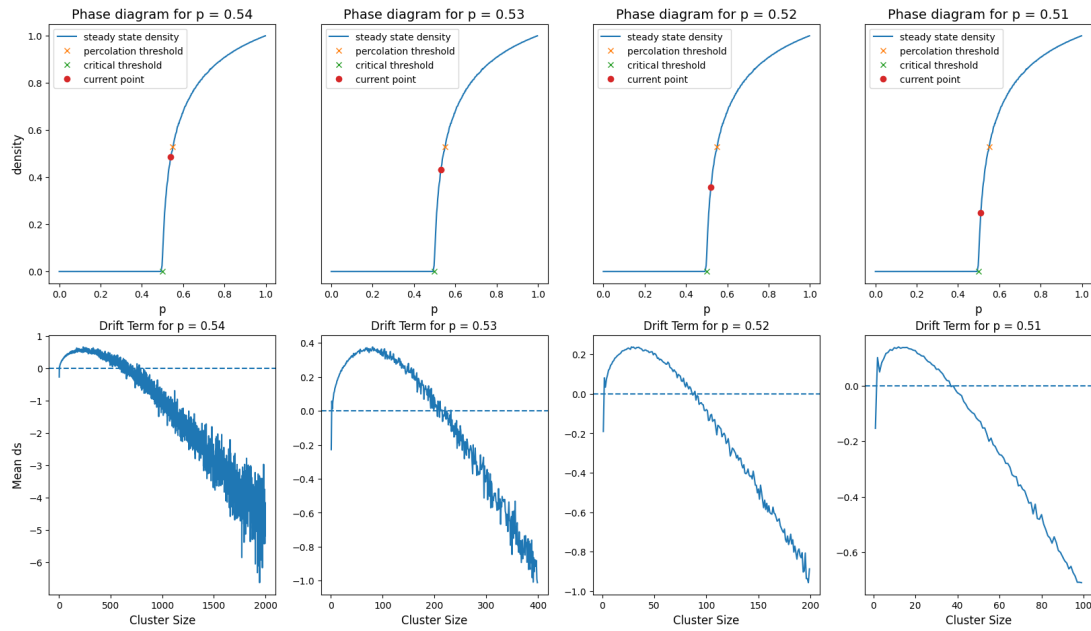


Figure 5.14: Variation in fixed point near the critical threshold of  $q = 0.5$

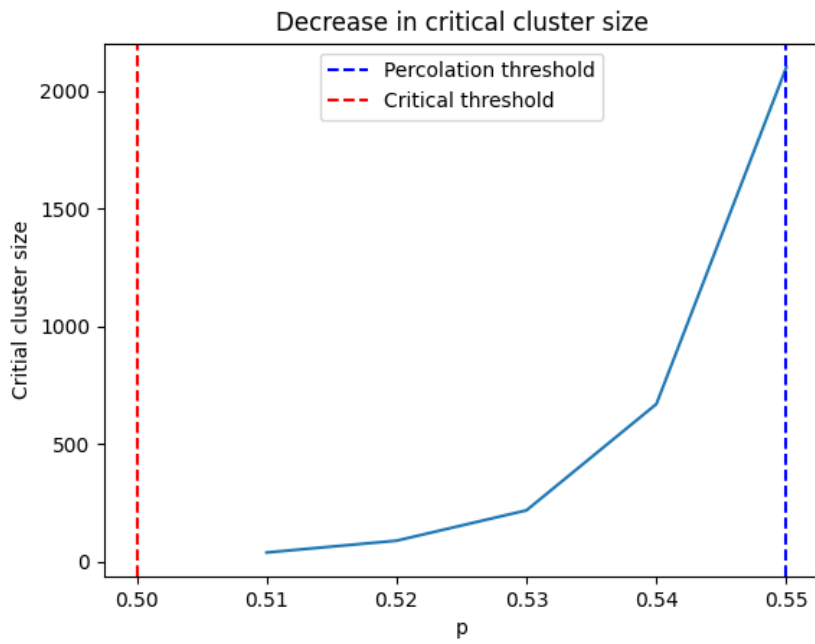


Figure 5.15: Decrease in critical cluster size near the critical threshold of  $q = 0.5$

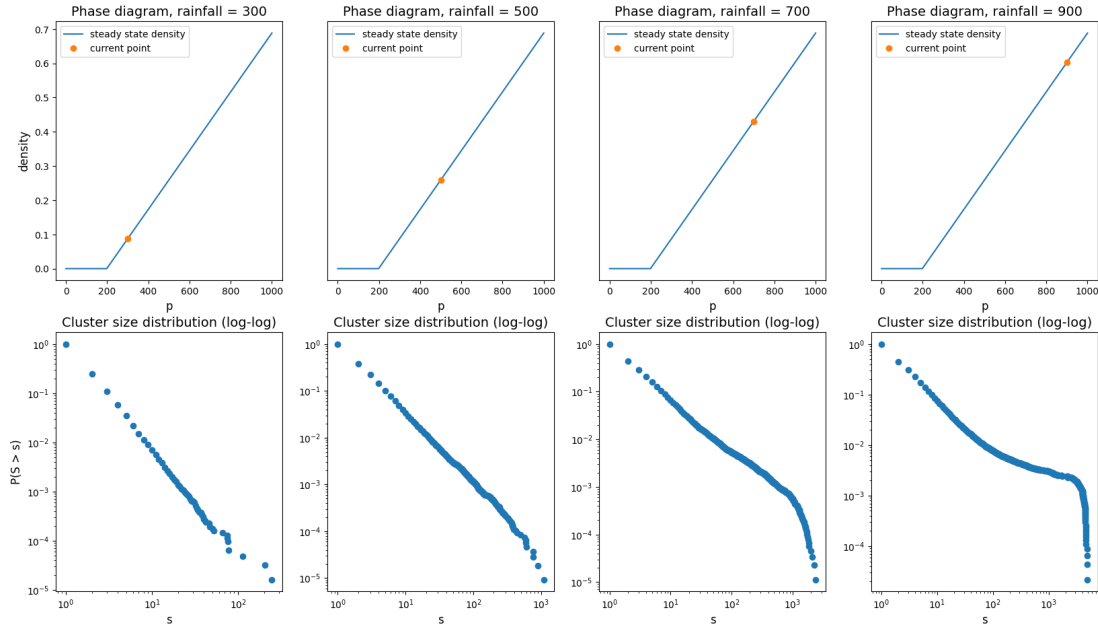


Figure 5.16: Cluster size distribution in Scanlon's model

## 5.4 Ubiquity of Power-Law Behaviour

Most of this thesis concentrates on the TDP model. This is because the TDP model is relatively simple. An occupied cell can only affect its Von-Neumann neighbours. However, we would like to show that other patchy ecosystem models also showcase a power-law behaviour in their cluster size distribution as well as their cluster dynamics. This is why we introduced Scanlon's model in 2.3.

Figure 5.16 describes the cluster size distribution in Scanlon's model, whereas 5.17 describes its cluster dynamics. These graphics look very similar to that of TDP model. Maybe the early warning signals discussion in sections 5.1 and 5.2 are applicable for Scanlon's model too.

Figure 5.18 showcases the drift (top graphs) and diffusion (bottom graphs) terms for Scanlon's model. These graphs are wildly different from that of TDP model. Besides, their interpretation remains elusive.

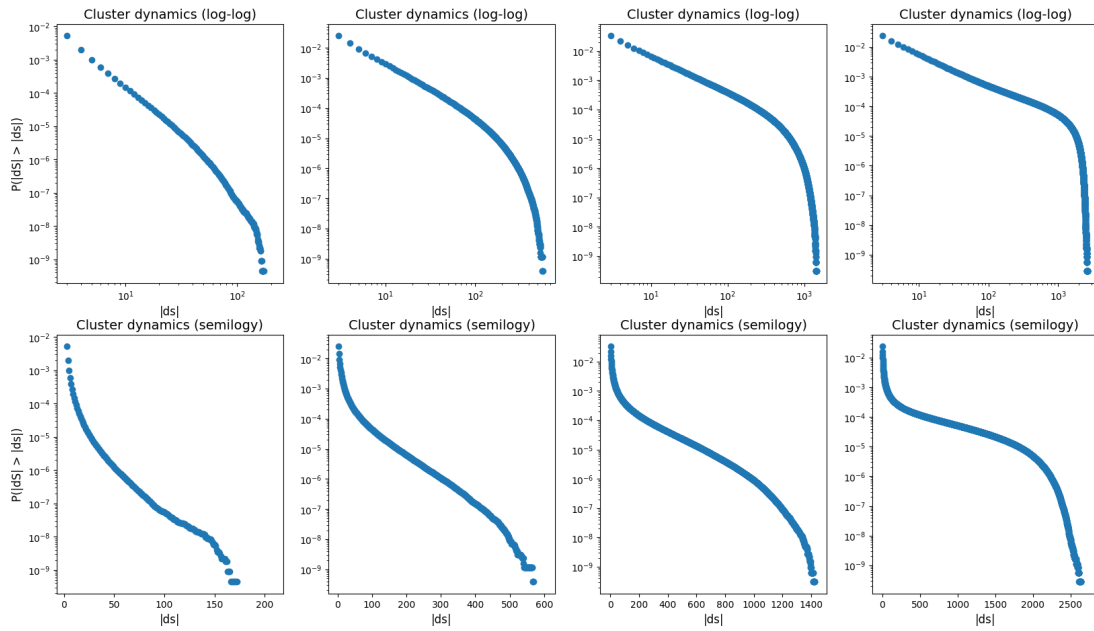


Figure 5.17: Cluster dynamics in Scanlon's model  
Left to right: rainfall = 300, 500, 700, 900

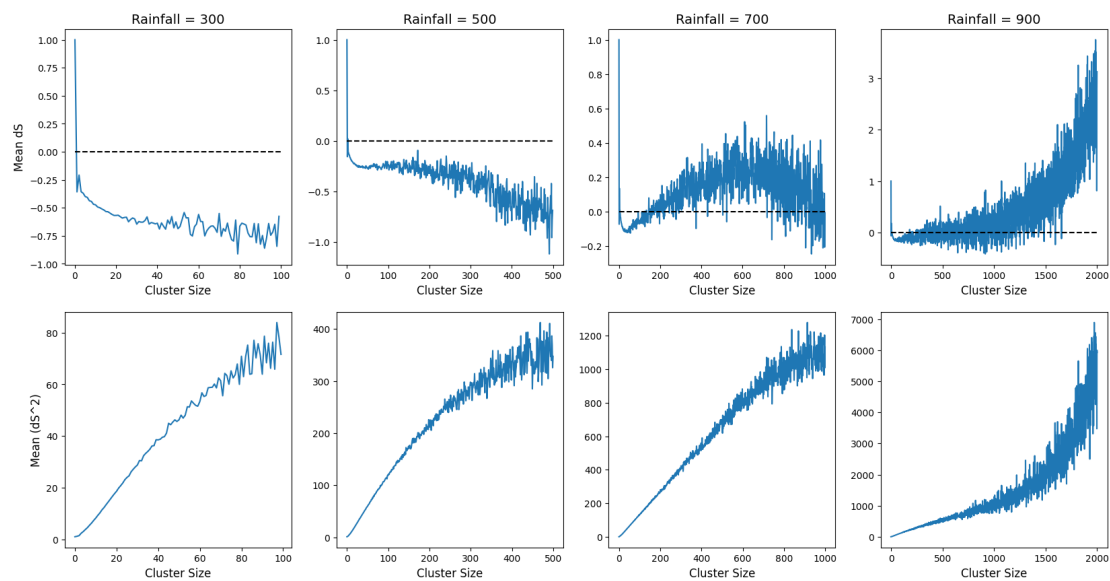


Figure 5.18: Drift and diffusion terms in Scanlon's model

## 5.5 Concluding Remarks and Future Work

The reasons for formulating early warning signals were made clear. The working of three models of patchy ecosystems were studied, alongside that of two null models. Their phase transitions and percolation properties were elucidated. Their simulations yielded us cluster size distributions and cluster dynamics, on the basis of which we were able to identify three early warning signals for patchy ecosystems (two of which are novel). Figure 5.19 summarises everything.

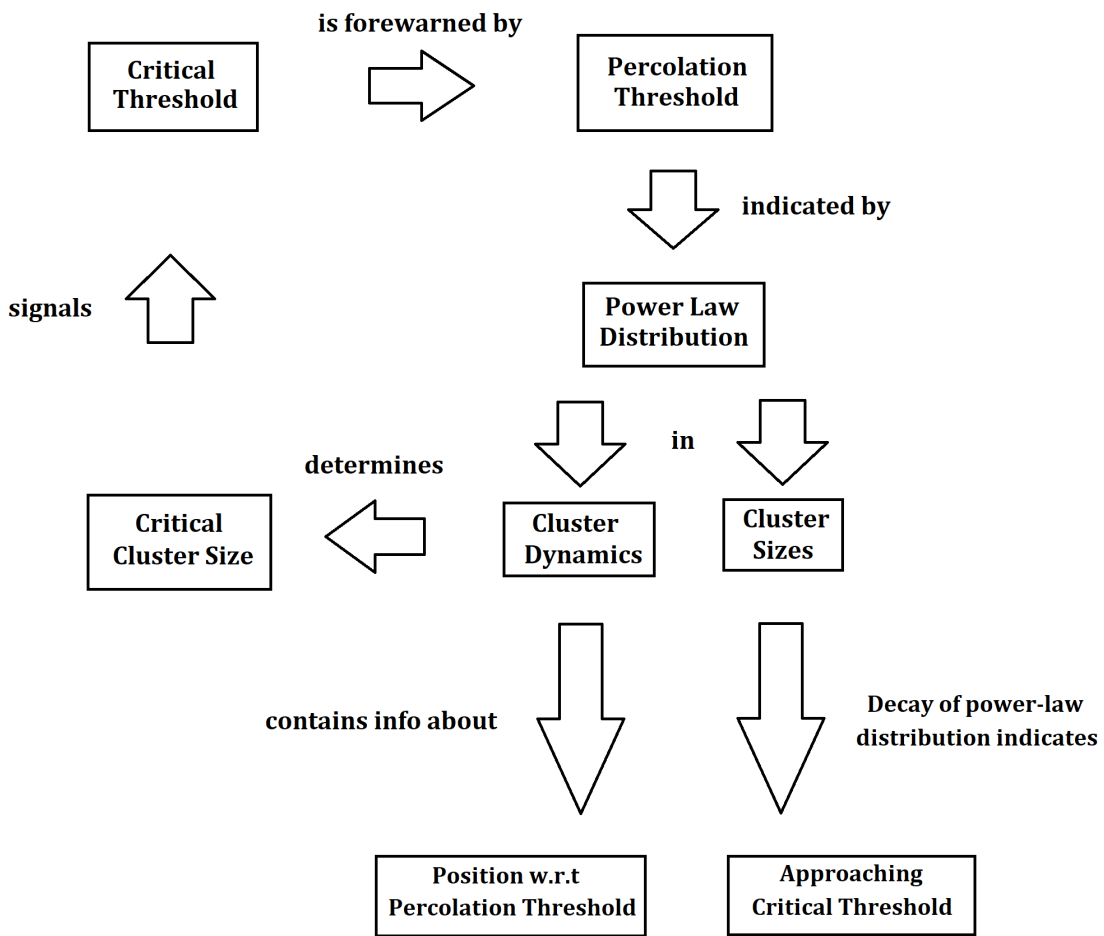


Figure 5.19: The global picture

We enumerate futures avenues that will be explored:

- Fitting of drift and diffusion terms:** While the diffusion term is relatively easy to fit, any fit of the drift term should not only capture the initial positive regime, but also the rapid decay afterwards. Moreover, the drift term for high levels of positive feedback has two fixed points instead of one. The drift term should ideally fit to an equation of the form  $y = ax - bx^2$ . The  $ax$  term is indicative of linear growth

for smaller cluster sizes. The  $-bx^2$  captures density dependent mortality for bigger clusters. However, second degree polynomial fits have failed to capture the intended dynamics. One can get an excellent fit using sixth degree polynomials. However, such actions amount to over-fitting, and the fits may not generalize well to higher values of cluster sizes (since higher order polynomials have a tendency to oscillate).

- b) **Analytical estimation of drift and diffusion terms:** By utilizing insights gained from approximating the drift and diffusion terms, one can attempt to arrive at functional forms from first principles. For an example, refer [Majumder et al. (2021)].
- c) **Self-consistency checking of SDEs:** Once the fitting of drift and diffusion terms in (a) is done properly, one can initialize clusters of several sizes (by sampling them from cluster distributions in a static null model), and evolve them according to the stochastic differential equation described in section 3.3:

$$\dot{x} = f(x) + g(x)\eta(t)$$

If the final distribution is similar to that of TDP model, then one can say that our drift and diffusion terms have accurately captured the dynamics of the model. This was attempted by using a sixth order polynomial fit of  $f(x)$ . We encountered numerical instabilities.

- d) **Solving Fokker-Planck equation:** This equation dictates the evolution of probability density  $p(x, t)$  of a dynamical variable  $x$  under the effect of drift and diffusion terms:

$$\frac{\partial p(x, t)}{\partial t} = -\frac{\partial}{\partial x}[f(x)p(x, t)] + \frac{1}{2}\frac{\partial^2}{\partial x^2}[g^2(x)p(x, t)]$$

Once the fitting of drift and diffusion terms in (a) is done properly, we can substitute them in the above equation. If the probability density of cluster sizes corresponding to a fixed point of this equation is similar to that of TDP model, then it confirms the accuracy of our drift and diffusion terms.

- e) **Application on empirical data:** A colleague of mine has compiled high resolution data of semi-arid ecosystems from different regions of the Kalahari transect, at different times. Rainfall gradients are suspected to exist across the spatial extent. We intend to apply the formulated early warning signals on this data.

All code and generated data that were utilized in this thesis can be found [here](#)

# Bibliography

- Clauset, A., Shalizi, C. R., and Newman, M. E. (2009). Power-law distributions in empirical data. *SIAM review*, 51(4):661–703.
- Génin, A., Majumder, S., Sankaran, S., Danet, A., Guttal, V., Schneider, F. D., and Kéfi, S. (2018). Monitoring ecosystem degradation using spatial data and the r package spatialwarnings. *Methods in Ecology and Evolution*, 9(10):2067–2075.
- Guttal, V. and Jayaprakash, C. (2008). Changing skewness: an early warning signal of regime shifts in ecosystems. *Ecology letters*, 11(5):450–460.
- Jhawar, J. and Guttal, V. (2020). Noise-induced effects in collective dynamics and inferring local interactions from data. *Philosophical Transactions of the Royal Society B*, 375(1807):20190381.
- Kéfi, S., Guttal, V., Brock, W. A., Carpenter, S. R., Ellison, A. M., Livina, V. N., Seekell, D. A., Scheffer, M., Van Nes, E. H., and Dakos, V. (2014). Early warning signals of ecological transitions: methods for spatial patterns. *PloS one*, 9(3):e92097.
- Kéfi, S., Rietkerk, M., Alados, C. L., Pueyo, Y., Papanastasis, V. P., ElAich, A., and De Ruiter, P. C. (2007a). Spatial vegetation patterns and imminent desertification in mediterranean arid ecosystems. *Nature*, 449(7159):213–217.
- Kéfi, S., Rietkerk, M., Roy, M., Franc, A., De Ruiter, P. C., and Pascual, M. (2011). Robust scaling in ecosystems and the meltdown of patch size distributions before extinction. *Ecology letters*, 14(1):29–35.
- Kéfi, S., Rietkerk, M., Van Baalen, M., and Loreau, M. (2007b). Local facilitation, bistability and transitions in arid ecosystems. *Theoretical population biology*, 71(3):367–379.
- Ludwig, D., Jones, D. D., Holling, C. S., et al. (1978). Qualitative analysis of insect outbreak systems: the spruce budworm and forest. *Journal of animal ecology*, 47(1):315–332.

- Majumder, S., Das, A., Kushal, A., Sankaran, S., and Guttal, V. (2021). Finite-size effects, demographic noise, and ecosystem dynamics. *The European Physical Journal Special Topics*, 230(16):3389–3401.
- Majumder, S., Tamma, K., Ramaswamy, S., and Guttal, V. (2019). Inferring critical thresholds of ecosystem transitions from spatial data. *Ecology*, 100(7):e02722.
- Manor, A. and Shnerb, N. M. (2008). Origin of pareto-like spatial distributions in ecosystems. *Physical Review Letters*, 101(26):268104.
- May, R. M. (1977). Thresholds and breakpoints in ecosystems with a multiplicity of stable states. *Nature*, 269(5628):471–477.
- Rietkerk, M., Boerlijst, M. C., van Langevelde, F., HilleRisLambers, R., de Koppel, J. v., Kumar, L., Prins, H. H., and de Roos, A. M. (2002). Self-organization of vegetation in arid ecosystems. *The American Naturalist*, 160(4):524–530.
- Sankaran, S., Majumder, S., Viswanathan, A., and Guttal, V. (2019). Clustering and correlations: Inferring resilience from spatial patterns in ecosystems. *Methods in Ecology and Evolution*, 10(12):2079–2089.
- Scanlon, T. M., Caylor, K. K., Levin, S. A., and Rodriguez-Iturbe, I. (2007). Positive feedbacks promote power-law clustering of kalahari vegetation. *Nature*, 449(7159):209–212.
- Scheffer, M., Carpenter, S., Foley, J. A., Folke, C., and Walker, B. (2001). Catastrophic shifts in ecosystems. *Nature*, 413(6856):591–596.
- Weissmann, H. and Shnerb, N. M. (2014). Stochastic desertification. *Europhysics Letters*, 106(2):28004.
- Weissmann, H. and Shnerb, N. M. (2016). Predicting catastrophic shifts. *Journal of theoretical biology*, 397:128–134.